Inorg. Chem. **2006**, *45*, 5852–5866

Comparative Bonding Behavior of Functional Cyclopentadienyl Ligands and Boron-Containing Analogues in Heterometallic Complexes and Clusters†

Pierre Croizat,‡ Nicolas Auvray,‡ Pierre Braunstein,*,‡ and Richard Welter§

Laboratoire de Chimie de Coordination, UMR 7177 CNRS, Université Louis Pasteur, 67070 Strasbourg Cédex, France, and Laboratoire DECOMET, UMR 7177 CNRS, Université Louis Pasteur, 67070 Strasbourg Cédex, France

Received February 24, 2006

The reactivity of isolobal molybdenum carbonylmetalates containing a 2-boratanaphthalene, $[Mo(\eta^5\text{-}2,4\text{-}MeC_9H_6BMe)(CO)_3]^-$ (**5a**) and $[Mo(\eta^5\text{-}2,4\text{-}MeC_9H_6BN\textit{i}\text{-}Pr_2)(CO)_3]^-$ (**5b**), a 1-boratabenzene, $[Mo(\eta^5\text{-}3,5\text{-}Me_2C_5H_3BN\textit{i}\text{-}Pr_2)(CO)_3]^-$ (**8**), or a functionalized cyclopentadienyl ligand, the new metalate $[Mo(\eta^5\text{-}C_5H_4Ph)(CO)_3]^-$ (**7**) and $[Mo(\eta^5\text{-}C_5H_4NMe_2)(CO)_3]^-$ (**9**), toward palladium (I and II) or platinum (I and II) complexes, such as *trans*-$[PdCl_2(NCPh)_2]$, $[Pd_2(NCMe)_6](BF_4)_2$, *trans*-$[PtCl_2(PEt_3)_2]$, and $[N(n\text{-}Bu)_4]_2[Pt_2Cl_4(CO)_2]$, has been investigated, and this has allowed an evaluation of the influence of the π-bonded ligands on the structures and unprecedented coordination modes observed in the resulting metal–metal-bonded heterometallic clusters. The new 58 CVE planar-triangulated centrosymmetric clusters, $[Mo_2Pd_2(\eta^5\text{-}C_5H_4Ph)_2(CO)_6(PEt_3)_2]$ (**11**), $[Mo_2Pd_2(\eta^5\text{-}2,4\text{-}MeC_9H_6BN\textit{i}\text{-}Pr_2)_2(CO)_6]$ (**12**), $[Mo_2Pd_2(\eta^5\text{-}3,5\text{-}Me_2C_5H_3BN\textit{i}\text{-}Pr_2)_2(CO)_6]$ (**13**), $[Mo_2Pd_2(\eta^5\text{-}C_5H_4NMe_2)_2(CO)_6(PEt_3)_2]$ (**15**), $[Mo_2Pt_2(\eta^5\text{-}C_5H_4NMe_2)_2(CO)_6(PEt_3)_2]$ (**16**), and $[Mo_2Pt_2(\eta^5\text{-}C_5H_4NMe_2)_2(CO)_8]$ (**20**), have been characterized by single-crystal X-ray diffraction. Their structural features were compared with those of the 54 CVE cluster $[Re_2Pd_2(\eta^5\text{-}C_4H_4BPh)_2(CO)_6]$ (**4**), previously obtained from the borole-containing metalate $[Re(\eta^5\text{-}C_4H_4BPh)(CO)_3]^-$ (**2**), in which a 2e–3c B–C_{ipso}–Pd interaction involving the π-ring was observed. As an extension of what has been observed in **4**, clusters **12** and **13** present a direct interaction of the boratanaphthalene (**12**) and the boratabenzene (**13**) ligands with palladium. In clusters **11**, **15**, **16**, and **20**, the π-ring does not interact with the palladium (**11** and **15**) or platinum centers (**16** and **20**), which confers to these clusters a geometry very similar to that of $[Mo_2Pd_2(\eta^5\text{-}C_5H_5)_2(CO)_6(PEt_3)_2]$ (**3b**). The carbonylmetalates $[Mo(\pi\text{-ring})(CO)_3]^-$ are thus best viewed as formal four electron donors which bridge a dinuclear d^9–d^9 unit. The orientation of this building block in the clusters influences the shape of their metal cores and the bonding mode of the bridging carbonyl ligands. The crystal structure of new centrosymmetric complex $[Mo(\eta^5\text{-}C_5H_4Ph)(CO)_3]_2$ (**10**) was determined, and it revealed intramolecular contacts of 2.773(4) Å between the carbon atoms of carbonyl groups across the metal–metal bond and intermolecular bifurcated interactions between the carbonyl oxygen atoms (2.938(4) and 3.029(4) Å), as well as intermolecular C–H$\cdots\pi_{Ar}$(C═C) interactions (2.334(3) and 2.786(4) Å) involving the phenyl substituents.

Introduction

The cyclopentadienide anion, $(C_5H_5)^-$, is one of the most important ligands in organometallic chemistry, and it has been associated with a number of metals to form a wide range of neutral or anionic reagents that have been used, in turn, for further organometallic synthesis. For example, this was used for the preparation of the first complex containing a heterometallic metal−metal bond.[1] A considerable number of dinuclear and cluster complexes have since been obtained from cyclopentadienyl-containing reagents, such as $[M(\eta^5\text{-}C_5H_5)(CO)_3]^-$ (M = Cr, **1a**; M = Mo, **1b**; M = W, **1c**). We have previously used the isolobal analogy between the cyclopentadienide anion and the 6π-electron borollide dianion $(C_4H_4BR)^{2-}$ (R = Ph) to compare the reactivity and

† Part of the PhD Thesis of P.C.

* To whom correspondence should be addressed. E-mail: braunst@chimie.u-strasbg.fr.

‡ Laboratoire de Chimie de Coordination.

§ Laboratoire DECOMET.

(1) Abel, E. W.; Singh, A.; Wilkinson, G. *J. Chem. Soc.* **1960**, 1321.

10.1021/ic060318d CCC: $33.50
Published on Web 06/29/2006

bonding behavior of the corresponding metal-centered organometallic nucleophiles of two adjacent columns of the Periodic Classification, such as **1** and $[Re(\eta^5\text{-}C_4H_4BR)(CO)_3]^-$ (**2**).[2]

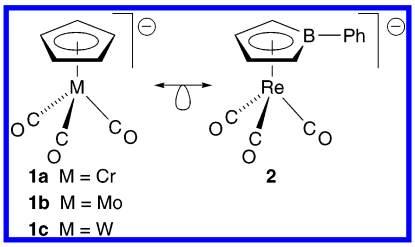

This was applied to the study of heterometallic metal−metal-bonded complexes and clusters and led to the discovery of unprecedented bonding situations. Thus, we found that the 58 cluster valence electron (CVE), planar, triangulated $[M_2Pd_2(\eta^5\text{-}C_5H_5)_2(CO)_6(PEt_3)_2]$ (M = Cr, **3a**; M = Mo, **3b**; M = W, **3c**)[3] clusters do not have direct analogues in the borole series since, despite its planar triangulated metal core characterized by the presence of 5 metal−metal bonds, the $[Re_2Pd_2(\eta^5\text{-}C_4H_4BPh)_2(CO)_6]$ (**4**) cluster contains only 54 CVE.[4] In this most unusual cluster, the borole ligand not only binds to rhenium in the usual η^5 manner but also to the adjacent palladium via a 2e−3c B−C_{ipso}−Pd system.

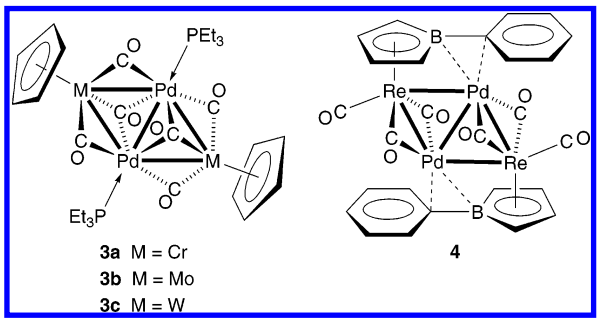

The intriguing similarities and differences between clusters **3** and **4** led us to extend our studies to the borole-containing carbonylmetalates, $[HFe(\eta^5\text{-}C_4H_4BPh)(CO)_2]^-$ [5,6] and $[Fe(\eta^5\text{-}C_4H_4BPh)(CO)_2CN]^-$,[7] and then to the 2-boratanaphthalene derivatives **5a** and **b**.[2]

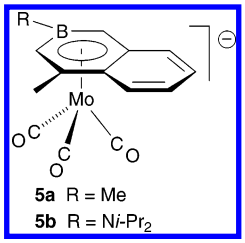

The boron-containing six-membered ring in **5a** and **5b** should behave as *monoanionic* 6π-electron donors, like the five-membered anionic $(\eta^5\text{-}C_5H_5)^-$ ligand and the five-membered *dianionic* 6π-electron donor borollide ligand. Consistently, the first metal cluster with a boratanaphthalene ligand, $[Mo_2Pd_2(\eta^5\text{-}2,4\text{-}MeC_9H_6BMe)_2(CO)_6(PEt_3)_2]$ (**6**),[2] was prepared from **5a** and shown to contain a planar, triangulated metal core with a center of symmetry in the middle of the Pd−Pd bond, similar to that in the $\eta^5\text{-}C_5H_5$ derivatives, **3**.[3]

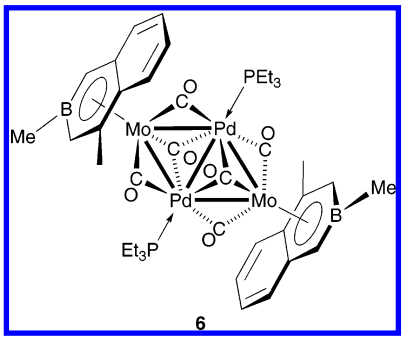

Although the original reaction of the 1,2-dimethoxyethane (DME) lithium salt of **5a** (Li·**5a**·2DME) with *trans*-$[PdCl_2(NCPh)_2]$ yielded a product with a deep blue color, characteristic of a metal−metal-bonded complex, perhaps a Mo_2Pd_2 cluster analogous to borole cluster **4**, it was too unstable to be identified.

Intrigued by the 2e−3c B−C_{ipso}−Pd bonding in cluster **4**, we wondered if a phenyl substituent on a π-donor ring system, other than a borole, could bring about this bonding behavior. This led us to study the reactivity of the phenyl-substituted cyclopentadienyl derivative $[Mo(\eta^5\text{-}C_5H_4Ph)(CO)_3]^-$ (**7**) toward palladium reagents (see below).

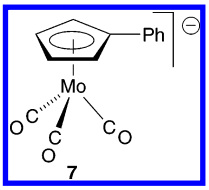

We then considered that a stronger donor substituent than phenyl, for example, an amino group, on the π-bonded ring of the molybdate reagent should be more efficient in providing the adjacent palladium centers with enough electron density and therefore in confering more stability to the product. Using the amino-substituted boratanaphthalene reagent **5b**, we have now been able to structurally characterize a Mo_2Pd_2 cluster in which, unexpectedly, the π-system of the boratanaphthalene ligand interacts with the Pd centers, rather than the amino group. We also turned our attention to related aminoboratabenzene and aminocyclopentadienyl ligands, and the results of our investigations with the corresponding isoelectronic carbonylmetalates, $[Mo(\eta^5\text{-}3,5\text{-}Me_2C_5H_3BN\text{-}i\text{-}Pr_2)(CO)_3]^-$ (**8**) and $[Mo(\eta^5\text{-}C_5H_4NMe_2)(CO)_3]^-$ (**9**), respectively, are described here.

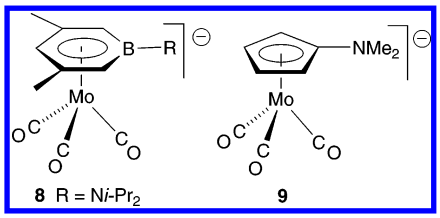

(2) Braunstein, P.; Cura, E.; Herberich, G. E. *J. Chem. Soc., Dalton Trans.* **2001**, 1754.
(3) Bender, R.; Braunstein, P.; Jud, J. M.; Dusausoy, Y. *Inorg. Chem.* **1983**, *22*, 3394.
(4) Braunstein, P.; Englert, U.; Herberich, G. E.; Neuschütz, M. *Angew. Chem., Int. Ed. Engl.* **1995**, *34*, 1010.

Scheme 1. Complexes and Clusters Containing Anionic 4-Electron Donor Ligands or Metalloligands Bridging a $R_3P \rightarrow d^9-d^9 \leftarrow PR_3$ Central Unit

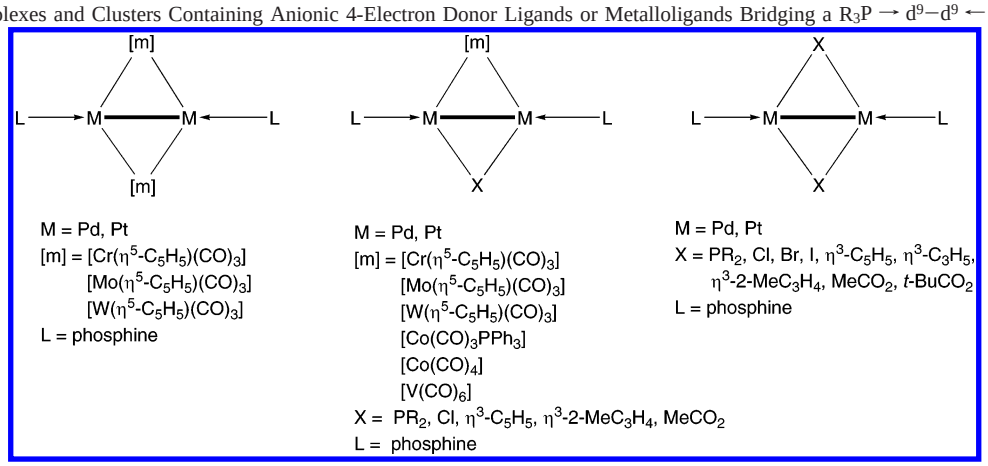

A structural comparison of the bonding of the various carbonylmetalate fragments in their respective clusters has also been performed. Since a localized electron count around each metal center (18e for Cr, Mo, or W and 16e for Pd or Pt) in clusters **3** and their platinum analogues is not straightforward, it has been found convenient to consider the whole anionic bridging moiety μ-[Mo(η^5-C_5H_5)$(CO)_3]^-$ as formally donating 4 electrons to the $R_3P \rightarrow Pd(I)-Pd(I) \leftarrow PR_3$ or $R_3P \rightarrow Pt(I)-Pt(I) \leftarrow PR_3$ ($R_3P \rightarrow d^9-d^9 \leftarrow PR_3$) unit. This confers to this 18e anionic fragment a bonding behavior related to that observed for the 4-electron donor bridging phosphido ligands (μ-PR_2^-) in some dinuclear Pd(I)[8−11] and Pt(I) complexes[12] or in trinuclear heterometallic platinum−molybdenum[13] and platinum−cobalt[14] clusters (Scheme 1). Furthermore, this bridging bonding mode can also be compared to that of a bridging halide (μ-X^-),[15−17] an allyl-ene type η^3-cyclopentadienide (μ-(η^3-C_5H_5)$^-$),[18−20] an η^3-allyl (μ-(η^3-C_3H_5)$^-$ and μ-(η^3-2-MeC_3H_4)$^-$),[17−21] or a carboxylate (μ-RCO_2^-) ligand[18−20] because they can also be considered to be anionic 4-electron donors toward the dinuclear unit $R_3P \rightarrow M-M \leftarrow PR_3$, where M is an ion with a d^9 electronic configuration (Scheme 1).

The isolobal analogy between these bridging fragments[22] encouraged us to explore its extension to other μ-[Mo(π-ring)$(CO)_3]^-$ metalloligands in metal clusters, and these aspects will also be examined here.

Results and Discussion

1. Mixed-Metal Palladium−Molybdenum Clusters. 1.1. Ph-Substituted Cp Derivatives. Inspired by the fact that the Re-coordinated phenyl-substituted borole ligand is able to generate a 2e−3c B−C_{ipso}−Pd system in cluster **4**, we prepared the new metalate [Mo(η^5-C_5H_4Ph)$(CO)_3]^-$ (**7**), by reaction between the sodium phenylcyclopentadienide Na-(C_5H_4Ph) and $[Mo(CO)_6]$, to determine if its phenyl-substituted cyclopentadienyl ligand[23] could give rise to a related 2e−3c $C_{ipsoCp}-C_{ipsoPh}$−Pd bonding interaction. Unfortunately, reactions between 2 equiv of the DME solvated sodium salt of **7** (Na·**7**·2DME) and *trans*-$[PdCl_2(NCPh)_2]$ or the Pd−Pd complex $[Pd_2(NCMe)_6](BF_4)_2$ [24] did not allow a stable, pure complex to be isolated. Separation of the reaction mixtures by column chromatography afforded the new homodinuclear complex [Mo(η^5-C_5H_4Ph)$(CO)_3]_2$ (**10**).

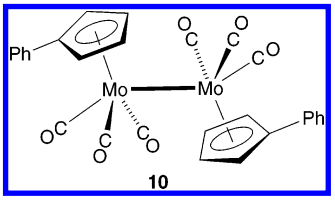

The formation of this complex results from a redox reaction, in agreement with general observations made in the course of our investigations on the syntheses of the Mo_2-Pd_2 clusters containing the Cp ligand.[3] An ORTEP view of the structure of **10** is shown in Figure 1 with the main distances and angles. The Mo−Mo distance of 3.2134(8) Å in this centrosymmetric dinuclear complex is close to that

(5) Braunstein, P.; Englert, U.; Herberich, G. E.; Neuschütz, M.; Schmidt, M. U. *J. Chem. Soc., Dalton Trans.* **1999**, 2807.
(6) Braunstein, P.; Herberich, G. E.; Neuschütz, M.; Schmidt, M. U.; Englert, U.; Lecante, P.; Mosset, A. *Organometallics* **1998**, *17*, 2177.
(7) Braunstein, P.; Herberich, G. E.; Neuschütz, M.; Schmidt, M. U. *J. Organomet. Chem.* **1999**, *580*, 66.
(8) Arif, A. M.; Heaton, D. E.; Jones, R. A.; Nunn, C. M. *Inorg. Chem.* **1987**, *26*, 4228.
(9) Sommovigo, M.; Pasquali, M.; Leoni, P.; Englert, U. *Inorg. Chem.* **1994**, *33*, 2686.
(10) Pasquali, M.; Sommovigo, M.; Leoni, P.; Sabatino, P.; Braga, D. *J. Organomet. Chem.* **1992**, *423*, 263.
(11) Leoni, P.; Pasquali, M.; Sommovigo, M.; Albinati, A.; Lianza, F.; Pregosin, P. S.; Ruegger, H. *J. Organomet. Chem.* **1995**, *488*, 39.
(12) Taylor, N. J.; Chieh, P. C.; Carty, A. J. *J. Chem. Soc., Chem. Commun.* **1975**, 448.
(13) Archambault, C.; Bender, R.; Braunstein, P.; Bouaoud, S.-E.; Rouag, D.; Golhen, S.; Ouahab, L. *Chem. Commun.* **2001**, 849.
(14) Bender, R.; Braunstein, P.; Metz, B.; Lemoine, P. *Organometallics* **1984**, *3*, 381.
(15) Vilar, R.; Mingos, D. M. P.; Cardin, C. J. *J. Chem. Soc., Dalton Trans.* **1996**, 4313.
(16) Durà Vilà, V.; Mingos, D. M. P.; Vilar, R.; White, A. J. P.; Williams, D. J. *J. Organomet. Chem.* **2000**, *600*, 198.
(17) Jolly, P. W.; Krueger, C.; Schick, K. P.; Wilke, G. *Z. Naturforsch.* **1980**, *35B*, 926.
(18) Werner, H.; Thometzek, P.; Krüger, C.; Kraus, H. J. *Chem. Ber.* **1986**, *119*, 2777.
(19) Thometzek, P.; Werner, H. *Organometallics* **1987**, *6*, 1169.
(20) Werner, H. *Adv. Organomet. Chem.* **1981**, *19*, 155.
(21) Krause, J.; Goddard, R.; Mynott, R.; Poerschke, K.-R. *Organometallics* **2001**, *20*, 1992.
(22) Hoffmann, R. *Angew. Chem., Int. Ed. Engl.* **1982**, *21*, 711.
(23) Riemschneider, R.; Nehring, R. *Monatsh. Chem.* **1960**, *91*, 829.
(24) Murahashi, T.; Nagai, T.; Okuno, T.; Matsutani, T.; Kurosawa, H. *Chem. Commun.* **2000**, 1689.

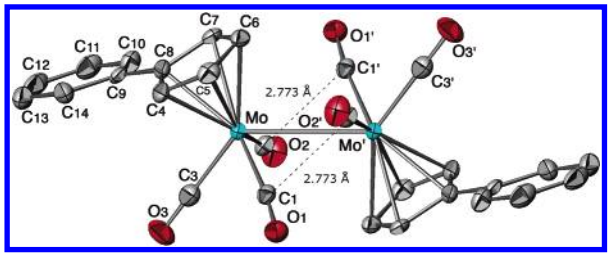

Figure 1. ORTEP view of the structure **10** with the atom-numbering scheme. Thermal ellipsoids enclose 50% of the electron density. Selected bond distances (Å) and angles (deg): Mo−Mo′ = 3.2134(8), Mo−C(1) = 1.983(3), Mo−C(2) = 1.987(3), Mo−C(3) = 1.972(3), C(1)−O(1) = 1.149(3), C(2)−O(2) = 1.146(3), C(3)−O(3) = 1.143(3); Mo−C(1)−O(1) = 172.1(3), Mo−C(2)−O(2) = 173.4(3), Mo−C(3)−O(3) = 179.1(3).

of 3.235(1) Å in $[Mo(\eta^5\text{-}C_5H_5)(CO)_3]_2$.[25] The angle between the mean planes of the cyclopentadienyl ring and its phenyl substituent is 18.8(1)°. Short intramolecular contacts, C(1)···C(2)′ and C(2)···C(1)′, of 2.773(4) Å are observed between the carbon atoms of carbonyl groups across the metal−metal bond (Figure 1), which are slightly shorter than those in $[Mo(\eta^5\text{-}C_5H_5)(CO)_3]_2$ (2.796(4) Å). Furthermore, intermolecular bifurcated interactions between the carbonyl oxygen atoms involve three adjacent molecules with O(1)···O(2) and O(1)···O(1) separations of 2.938(4) and 3.029(4) Å, respectively (Figure S-1 of the Supporting Information), while intermolecular C−H···π_{Ar}(C═C) interactions (2.334(3) and 2.786(4) Å) involve the phenyl substituents (Figure S-2).

The reaction of Na·**7**·2DME with *trans*-$[PdCl_2(PEt_3)_2]$ or with $[Pd_2(NCMe)_6](BF_4)_2$ in the presence of PEt_3, led to the formation of the $[Mo_2Pd_2(\eta^5\text{-}C_5H_4Ph)_2(CO)_6(PEt_3)_2]$ (**11**) cluster, X-ray diffraction analysis of which confirmed a centrosymmetric structure of the type found in **3**.

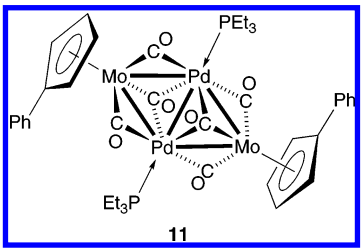

11

An ORTEP view of the structure of **11** is shown in Figure 2 with the main distances and angles. Each Mo atom is bonded to two asymmetric doubly bridging and one semi-triply bridging carbonyls. The mean planes of the C_5 rings are parallel by symmetry and form a dihedral angle, β, of 78.9(2)° with the metallic plane and an angle of 19.9(2)° with the mean plane of their phenyl substituents (see Table 1 and Scheme 2). A comparison with the $\eta^5\text{-}C_5H_5$ analogue **3b** shows that the presence of the phenyl ring does not influence the orientation of the π-bonded ligand $\eta^5\text{-}C_5H_4Ph$ with respect to the metal core, as shown by the values of the angles β and γ (between the axis passing through the π-ring centroid (C_{ring}) and the center of symmetry of the cluster (C_{sym}) and the M(2)M(2)′ axis; see Table 1 and Scheme 2). Coordination of the phosphine ligands to palladium is much favored over the formation of a 2e−3c C_{ipsoCp}−C_{ipsoPh}−Pd bonding system.

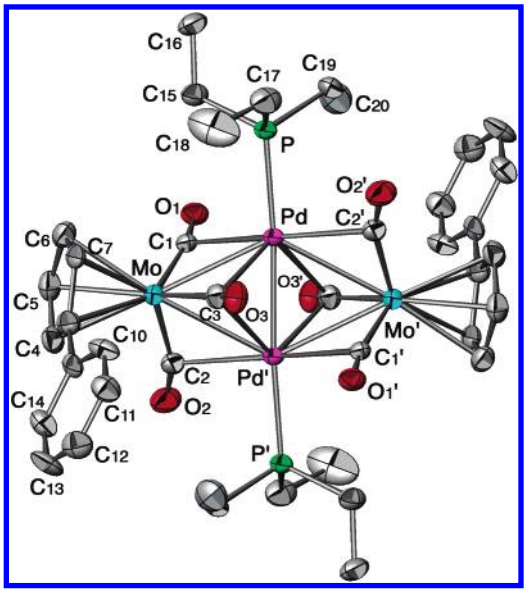

Figure 2. ORTEP view of the structure **11** with the atom-numbering scheme. Thermal ellipsoids enclose 50% of the electron density. Selected bond distances (Å) and angles (deg): Pd−Pd′ = 2.5836(9), Pd−Mo = 2.8128(9), Pd′−Mo = 2.8564(8), Pd−P = 2.328(2), Pd−C(1) = 2.374(6), Pd−C(2) = 2.370(7), Pd−C(3) = 2.283(6), Pd′−C(3) = 2.438(6), Mo−C(1) = 1.955(6), Mo−C(2) = 1.953(6), Mo−C(3) = 2.028(7), C(1)−O(1) = 1.184(6), C(2)−O(2) = 1.186(7), C(3)−O(3) = 1.175(7), C(8)−C(9) = 1.479(8); Pd′−Pd−Mo = 63.75(4), Mo−Pd−Mo′ = 125.78(3), Pd−Pd′−Mo = 62.03(3), Pd−Mo−Pd′ = 54.22(3), Pd′−Pd−P = 175.76(6), Mo−C(1)−O(1) = 166.6(5), Mo−C(2)−O(2) = 159.5(6), Mo−C(3)−O(3) = 158.4(5), Pd−C(1)−O(1) = 113.0(4), Pd−C(2)−O(2) = 118.2(5), Pd−C(3)−O(3) = 116.4(5), Pd′−C(3)−O(3) = 118.6(5).

Table 1. Structural Parameters

	β (deg)[a]	γ (deg)[b]	δ (deg)[c]	h (Å)[d]
23			1.95(10)	1.14(1)
3b	74.7(1)	87.19(1)	3.3(2)	0.90(1)
4	88.4(4)	68.33(4)	10.7(7)	1.01(1)
6	81.3(1)	86.06(1)	4.6(1)	0.91(1)
11	78.9(2)	87.05(2)	2.9(2)	0.89(1)
12	89.3(1)	74.72(2)	8.7(2)	1.06(1)
13	87.69(5)	68.99(1)	6.81(7)	1.10(1)
15	82.7(1)	85.14(3)	5.6(1)	0.86(1)
16	86.8(3)	86.54(3)	6.5(1)	0.83(1)
20	89.7(2)	75.87(1)	7.3(3)	1.02(1)

[a] β = angle between the metallic plane and the mean plane defined by the carbon atoms of the π-ring (Scheme 2). [b] γ = M(2)−C_{sym}−C_{ring} angle (Scheme 2). [c] δ = angle between the mean plane defined by the carbon atoms of the π-ring and the plane defined by the carbon atoms of the carbonyls. [d] h = shortest distance between M and the C(1)C(2)C(3) plane (Scheme 6).

1.2. Boratanaphthalene Derivatives. After studying the reaction of Li·**5a**·2DME with *trans*-$[PdCl_2(NCPh)_2]$ in the presence of PEt_3, which yielded $[Mo_2Pd_2(\eta^5\text{-}2,4\text{-}MeC_9H_6\text{-}BMe)_2(CO)_6(PEt_3)_2]$ (**6**), we examined the reaction of the amino-substituted reagent Li·**5b**·2DME with the dinuclear complex $[Pd_2(NCMe)_6](BF_4)_2$ in which the palladium is already in the +I oxidation state, as in the desired product, which should limit or suppress undesirable redox side-reactions. This led to the new cluster $[Mo_2Pd_2(\eta^5\text{-}2,4\text{-}MeC_9H_6BN\textit{i}\text{-}Pr_2)_2(CO)_6]$ (**12**) whose structure was determined by X-ray diffraction. An ORTEP view of the structure of **12** is shown in Figure 3 with the main distances and angles. Although we anticipated the presence of a 2e−3c B−N−Pd bonding, related to the 2e−3c B−C−Pd system

(25) Adams, R. D.; Collins, D. M.; Cotton, F. A. *Inorg. Chem.* **1974**, *13*, 1086.

Scheme 2. Representation of the Angles β and γ

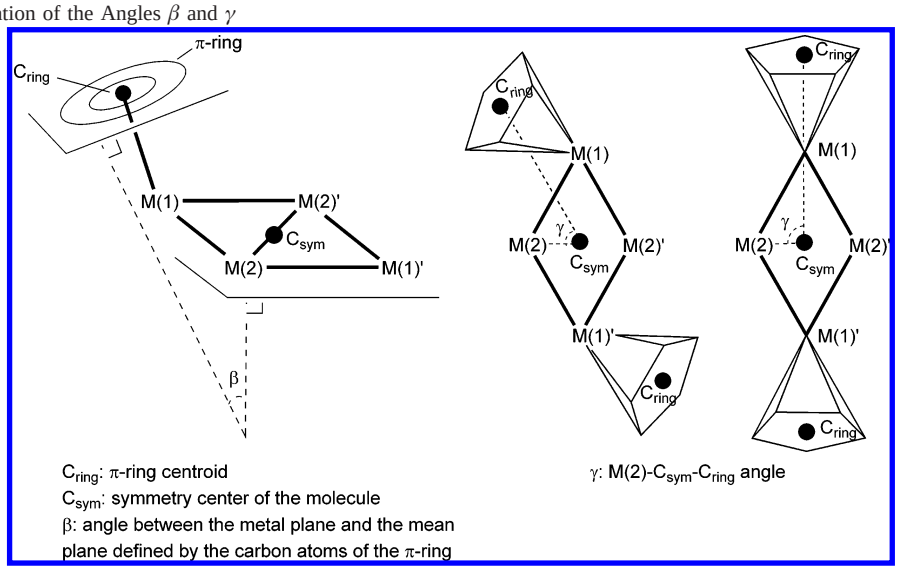

Scheme 3. Two Dispositions of the *meso*-Isomer of **12** Resulting in Disorder in the Crystal

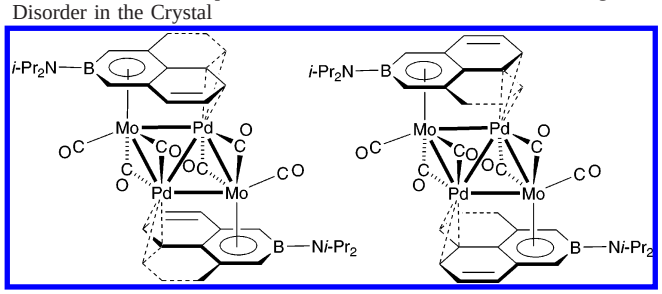

encountered in **4**, it is now the π-system of the aromatic ligand that donates electron density to the palladium centers.

The molecular structure possesses crystallographic centrosymmetry and displays disordered aminoboratanaphthalene ligands. This disorder relates to the bonding of the metal to the two enantiotopic faces of the planar chiral boratanaphthalene and is illustrated for the meso isomer in Scheme 3.

The apparent lateral symmetry of the metal-to-ligand bonding results from the superposition of the two alternative arrangements of the molecule. This superposition may equally well include the two racemic isomers. The planar geometry around the nitrogen atom of the BN*i*-Pr$_2$ group is shown by the sum of the angles around N of 360(1)°, which is consistent with a partial boron−nitrogen double bond (B−N = 1.413(6) Å).[26] There is no interaction between this group and the Pd centers. Each Mo center is bonded to one terminal and two semi-bridging carbonyls, as observed for cluster **4**. The mean planes defined by the carbon atoms of the boratanaphthalene ligands are, by symmetry, parallel to each other and form a dihedral angle, β, of 89.3(1)° with the metallic plane (see Table 1). The total valence electron count of this cluster is 58e, when including the two electrons donated to each Pd center by the boratanaphthalene π-system.

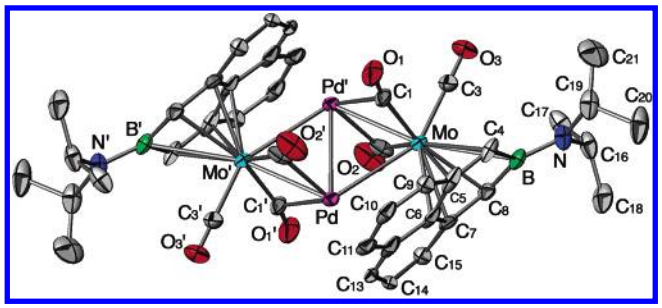

Figure 3. ORTEP view of the structure **12** with the atom-numbering scheme. Thermal ellipsoids enclose 50% of the electron density. For the disorder of the aminoboratanaphthalene ligands, see text. Selected bond distances (Å) and angles (deg): Pd−Pd′ = 2.892(1), Pd−Mo = 2.666(1), Pd′−Mo = 2.959(10), Pd−C(11) = 2.407(5), Pd−C(12) = 2.210(4), Pd−C(1) = 2.227(4), Pd−C(2) = 2.229(5), Mo−C(1) = 2.010(4), Mo−C(2) = 2.007(4), Mo−C(3) = 2.001(5), C(1)−O(1) = 1.167(5), C(2)−O(2) = 1.170(5), C(3)−O(3) = 1.135(5), B−N = 1.413(6); Pd′−Pd−Mo = 64.19(2), Mo−Pd−Mo′ = 118.38(2), Pd−Pd′−Mo = 54.20(3), Pd−Mo−Pd′ = 61.62(2), Mo−C(1)−O(1) = 163.5(4), Mo−C(2)−O(2) = 163.7(5), Mo−C(3)−O(3) = 179.9(5), Pd−C(1)−O(1) = 118.8(3), Pd−C(2)−O(2) = 118.5(4), B−N−C(16) = 123.5(3), B−N−C(19) = 122.2(3), C(16)−N−C(19) = 114.3(3).

1.3. Amino-boratabenzene Derivatives. We then considered it to be of interest to examine a similar reaction using the amino-substituted boratabenzene analogue of **5b**, [Mo(η^5-3,5-Me$_2$C$_5$H$_3$BN*i*-Pr$_2$)(CO)$_3$]$^-$ (**8**),[27] which is much less likely to lead to an interaction between the aromatic C=C system and the Pd centers. The reaction of 2 equiv of the DME-solvated lithium salt of **8** (Li·**8**·2DME)[27] with [Pd$_2$(NCMe)$_6$](BF$_4$)$_2$ in toluene produced the tetranuclear cluster [Mo$_2$Pd$_2$(η^5-3,5-Me$_2$C$_5$H$_3$BN*i*-Pr$_2$)$_2$(CO)$_6$] (**13**), and its crystal structure determination established the presence of a 2e−3c B−N−Pd bonding.

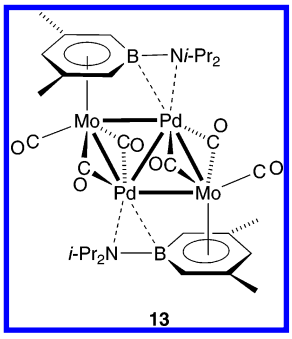

An ORTEP view of the structure of **13** is shown in Figure 4 with the main distances and angles. The B−Pd distance of 2.488(2) Å is shorter than the 2.59(2) Å observed in the

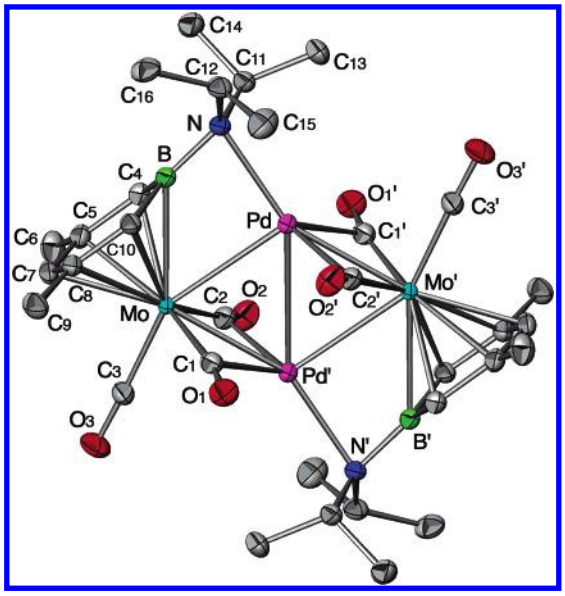

Figure 4. ORTEP view of the structure of **13** with the atom-numbering scheme. Thermal ellipsoids enclose 50% of the electron density. Selected bond distances (Å) and angles (deg): Pd−Pd′ = 3.015(1), Pd′−Mo = 2.676(1), Pd−Mo = 2.877(2), Pd−N = 2.304(2), Pd−B = 2.488(2), Pd−C(1) = 2.199(2), Pd−C(2) = 2.186(2), Mo−C(1) = 2.021(2), Mo−C(2) = 2.020(2), Mo−C(3) = 1.964(2), C(1)−O(1) = 1.173(3), C(2)−O(2) = 1.163(3), C(3)−O(3) = 1.175(3), B−N = 1.470(3); Pd−Pd′−Mo = 60.39(4), Mo−Pd−Mo′ = 114.35(4), Pd′−Pd−Mo = 53.96(4), Pd−Mo−Pd′ = 65.65(4), Mo−C(1)−O(1) = 164.4(2), Mo−C(2)−O(2) = 163.3(2), Mo−C(3)−O(3) = 178.0(2), Pd−C(1)−O(1) = 117.0(2), Pd−C(2)−O(2) = 117.8(2), N−Pd−Mo = 91.55(6), B−N−Pd = 79.09(11), B−N−C(11) = 116.8(2), B−N−C(12) = 120.3(2), C(11)−N−C(12) = 112.8(2).

case of **4**. The N−Pd distance is 2.304(2) Å. The angle, β, between the mean plane defined by the carbon atoms of the boratabenzene ring and the metal plane is 87.69(5)° (see Table 1). Because of its coordination to palladium, the environment of the nitrogen atom is not planar (sum of the angles around N = 349.9(4)°). Each molybdenum is bonded to a terminal carbonyl ligand and to two doubly bridging carbonyls. When the ligand η^5-3,5-$Me_2C_5H_3BN$*i*-Pr_2 is considered as a neutral moiety, it formally donates 5 electrons to the Mo and 2 to the adjacent Pd centers. This provides a total electron count of 58 for this cluster, similar to that in **3** but in contrast to the situation in **4**.

1.4. Amino-Cp Derivatives. For comparison with the amino-boratabenzene reagent **8** and to compare the bonding of the phenyl-borole ligand in **4** with that of a related Cp derivative, we used the metalate Li[Mo(η^5-$C_5H_4NMe_2$)-$(CO)_3$]·2DME (Li·**9**·2DME).[27] It was prepared by reaction of Li($C_5H_4NMe_2$) with [Mo$(CO)_6$] in refluxing DME and reacted with [$Pd_2(NCMe)_6$](BF_4)$_2$ in THF at −78 °C. A deep-blue solution was instantaneously formed, suggesting the formation of a mixed-metal complex, but unfortunately, various workup procedures only led to the formation of palladium (black) and of some red homodinuclear complex

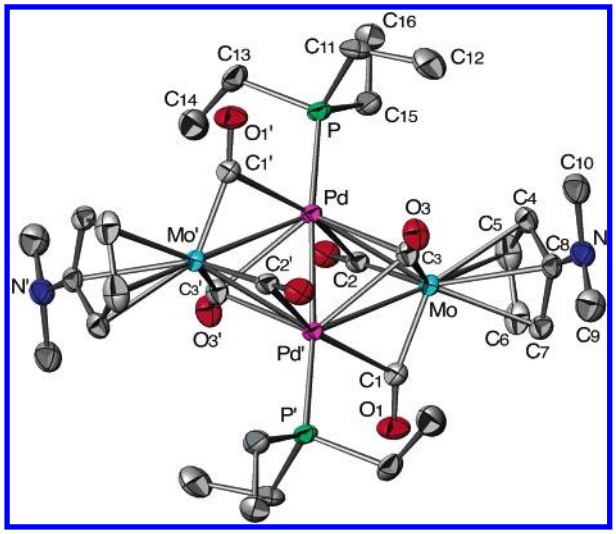

Figure 5. ORTEP view of the structure of **15** with the atom-numbering scheme. Thermal ellipsoids enclose 50% of the electron density. Selected bond distances (Å) and angles (deg): Pd−Pd′ = 2.590(2), Pd−Mo = 2.8075(5), Pd′−Mo = 2.867(1), Pd−P = 2.320(2), Pd−C(1) = 2.392(3), Pd−C(2) = 2.395(4), Pd−C(3) = 2.370(4), Pd′−C(3) = 2.480(4), Mo−C(1) = 1.972(4), Mo−C(2) = 1.977(4), Mo−C(3) = 2.033(3), C(1)−O(1) = 1.170(4), C(2)−O(2) = 1.165(4), C(3)−O(3) = 1.169(4), C(8)−N = 1.364(5); Pd′−Pd−Mo = 64.03(4), Mo−Pd−Mo′ = 125.71(5), Pd−Pd′−Mo = 61.68(4), Pd−Mo−Pd′ = 54.29(5), Pd′−Pd−P = 173.69(3), Mo−C(1)−O(1) = 157.4(3), Mo−C(2)−O(2) = 164.8(3), Mo−C(3)−O(3) = 159.9(3), Pd−C(1)−O(1) = 121.0(3), Pd−C(2)−O(2) = 115.8(3), Pd−C(3)−O(3) = 117.5(3), Pd′−C(3)−O(3) = 118.5(3), C(8)−N−C(9) = 119.0(3), C(8)−N−C(10) = 117.8(4), C(9)−N−C(10) = 117.0(3).

[Mo(η^5-$C_5H_4NMe_2$)$(CO)_3$]$_2$ (**14**) (IR (CH_2Cl_2) ν(CO): 1938s, 1898s cm^{-1}).

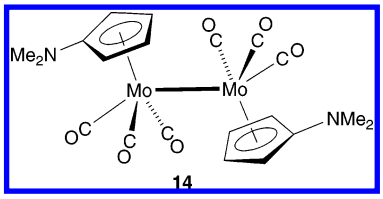

However, when the reaction was performed in the presence of 2 equiv of PEt_3, the reaction mixture became violet instantaneously, characteristic of a cluster of type **3**. Indeed, the new cluster isolated, [Mo_2Pd_2(η^5-$C_5H_4NMe_2$)$_2$$(CO)_6$-$(PEt_3)_2$] (**15**), was shown by X-ray diffraction to adopt a centrosymmetric structure.

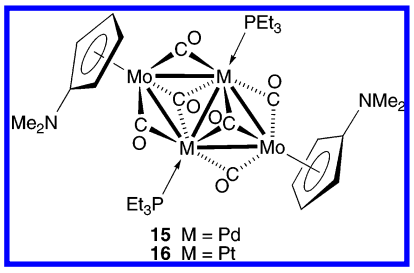

An ORTEP view of the structure of **15** is shown in Figure 5 with the main distances and angles. The angle, β, between the mean plane of the amino-cyclopentadienyl ligand and the metal plane is 82.7(1)° (see Table 1). The sum of the angles around N is 353.8(10)°.

(26) Allen, F. H.; Kennard, O.; Watson, D. G.; Brammer, L.; Orpen, A. G.; Taylor, R. *J. Chem. Soc., Perkin Trans. 2* **1987**, S1.
(27) Auvray, N.; Baul, T. B.; Braunstein, P.; Croizat, P.; Englert, U.; Herberich, G. E.; Welter, R. *Dalton Trans.* **2006**, 2950.

2. Mixed-Metal Platinum−Molybdenum Clusters

In view of the difficulty or impossibility of isolating some of the desired palladium-containing clusters because of their high lability or instability, we decided to explore the behavior of platinum analogues since platinum complexes and clusters are generally more stable than their palladium counterparts. By analogy with the successful use of $[Pd_2(NCMe)_6](BF_4)_2$ in the synthesis of heterometallic palladium clusters (see above), we decided first to prepare an analogous homodinuclear Pt(I) complex and explore its reactivity with the carbonylmetalates. The selective reduction of a Pt(II) precursor into a Pt(I) complex often remains an interesting challenge. Although homodinuclear Pt(I) complexes containing phosphine or isonitrile ligands are known,[28,29] we did not consider them to be suitable candidates since the strong phosphorus−platinum or carbon−platinum bonds, respectively, would not allow coordination of a weaker donor function in the final cluster. Preliminary experiments using $[N(n\text{-}Bu)_4]_2[Pt_2Cl_4(CO)_2]$[30] and Li·**9**·2DME were unsuccessful (see below). A desirable precursor with labile ligands coordinated to the metals would be $[Pt_2(NCMe)_6](BF_4)_2$ but this complex has not been described in the literature. We attempted to synthesize it by the reaction between $[Pt_2(dba)_3]$ and $[Pt(NCMe)_4](BF_4)_2$, following a procedure similar to that described for the synthesis of $[Pd_2(NCMe)_6](BF_4)_2$.[24] However, no reaction occurred at room temperature and decomposition to platinum metal was observed upon heating (even upon changing reaction conditions, solvents, temperature, etc.). Although SmI_2 is a convenient and mild one-electron reducing agent which changes color from purple to yellow upon oxidation to Sm(III),[31,32] its reactions with *trans*-$[PtCl_2(NCPh)_2]$ or *trans*-$[PtCl_2(NCMe)_2]$ in the corresponding organonitrile as a solvent at −20 °C, followed by the addition of NH_4PF_6, did not lead to the desired Pt(I)−Pt(I) complex. Decomposition to Pt metal was again observed at room temperature.

When the complex $[N(n\text{-}Bu)_4]_2[Pt_2Cl_4(CO)_2]$ was reacted with Li·**9**·2DME in THF at −78 °C, a deep-blue solution was obtained (ca. 1 h), but at higher temperature, rapid formation of platinum black and of **14** was observed. This color change suggests, like in the reaction of $[Pd_2(NCMe)_6](BF_4)_2$ with Li·**9**·2DME in the absence of phosphine, that cluster formation occurs but we cannot determine if it is accompanied by coordination of the amino-Cp ligand to the d^9 metal centers. Possible reaction intermediates are discussed below.

When *trans*-$[PtCl_2(PEt_3)_2]$ was reacted with 2 equiv of Li·**9**·2DME in THF at room temperature, the stable cluster $[Mo_2Pt_2(\eta^5\text{-}C_5H_4NMe_2)_2(CO)_6(PEt_3)_2]$ (**16**) was obtained and characterized by X-ray diffraction. An ORTEP view of the structure of **16** is shown in Figure 6 with the main distances and angles. This cluster adopts a centrosymmetric structure, similar to that of its palladium analogue **15** and to that of the 58 CVE, planar, triangulated cluster $[Mo_2Pt_2(\eta^5\text{-}C_5H_5)_2(CO)_6(PEt_3)_2]$.[33] Each Mo atom is bonded to three asymmetrically doubly bridging carbonyls, whereas two asymmetrically doubly bridging and one semi-triply bridging carbonyls were observed in **15** and $[Mo_2Pt_2(\eta^5\text{-}C_5H_5)_2(CO)_6(PEt_3)_2]$.[33] The coordination environment around the nitrogen atom is almost planar (sum of the angles around N of 354(3)°).

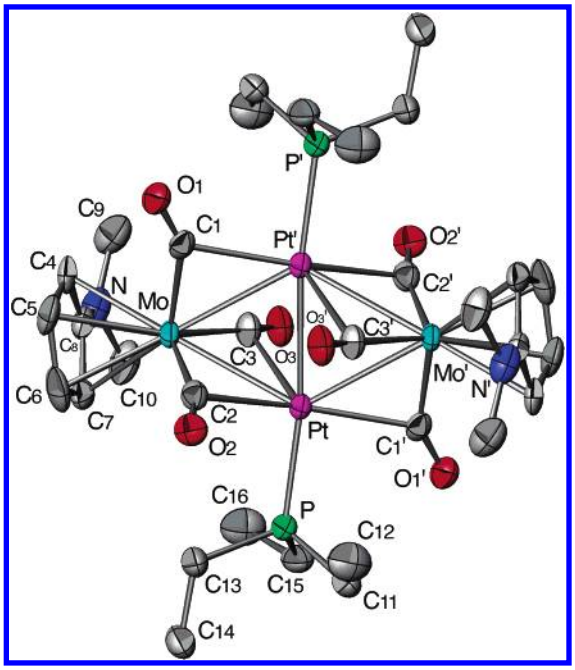

Figure 6. ORTEP view of the structure of **16** with the atom-numbering scheme. Thermal ellipsoids enclose 50% of the electron density. Selected bond distances (Å) and angles (deg): Pt−Pt′ = 2.650(2), Pt−Mo = 2.7739(8), Pt′−Mo = 2.826(2), Pt−P = 2.275(3), Pt−C(1) = 2.243(9), Pt−C(2) = 2.324(9), Pt−C(3) = 2.43(1), Mo−C(1) = 2.00(1), Mo−C(2) = 1.97(1), Mo−C(3) = 2.032(9), C(1)−O(1) = 1.16(1), C(2)−O(2) = 1.18(1), C(3)−O(3) = 1.16(1), C(8)−N(2) = 1.35(1); Pt′−Pt−Mo = 62.76(4), Mo−Pt−Mo′ = 123.52(6), Pt−Pt′−Mo = 60.76(4), Pt−Mo−Pt′ = 56.48(6), Pt′−Pt−P = 172.28(6), Mo−C(1)−O(1) = 149.3(8), Mo−C(2)−O(2) = 162.9(8), Mo−C(3)−O(3) = 164.7(8), Pt−C(1)−O(1) = 127.4(8), Pt−C(2)−O(2) = 116.7(7), Pt−C(3)−O(3) = 116.4(7), C(8)−N−C(9) = 118.6(10), C(8)−N−C(10) = 119.7(10), C(9)−N−C(10) = 115.6(10).

These results show that coordination of the phosphine ligands to palladium is much favored over a 2e−3c C_{ipsoCp}−N−Pd bonding situation.

3. Suggested Mechanism for the Formation of the Heterometallic Clusters. Formation of the heterotetranuclear clusters by reactions of the dinuclear precursor complexes $[Pd_2(NCMe)_6](BF_4)_2$ and $[N(n\text{-}Bu)_4]_2[Pt_2Cl_4(CO)_2]$ (in which the d^9−d^9 bond present in the product already exists) with the various carbonylmetalates could occur according to Scheme 4. Substitution of the MeCN or Cl ligands, respectively, would lead to deeply colored and reactive linear [m]−d^9−d^9−[m] intermediates ([m] = $Cr(\eta^5\text{-}C_5H_5)(CO)_3$, $Mo(\eta^5\text{-}C_5H_5)(CO)_3$, or $W(\eta^5\text{-}C_5H_5)(CO)_3$). These would rearrange upon addition of phosphine (**3b**, **6**, **11**, **15**, and **16**) or through direct coordination of the metalate ring (**12**

(28) Müller, T. E.; Ingold, F.; Menzer, S.; Mingos, D. M. P.; Williams, D. J. *J. Organomet. Chem.* **1997**, *528*, 163.
(29) Garrou, P. E. *Chem. Rev.* **1985**, *85*, 171.
(30) Goggin, P. L.; Goodfellow, R. J. *J. Chem. Soc., Dalton Trans.* **1973**, 2355.
(31) Ogoshi, S.; Morita, M.; Inoue, K.; Kurosawa, H. *J. Organomet. Chem.* **2004**, *689*, 662.
(32) Molander, G. A.; Harris, C. R. *Chem. Rev.* **1996**, *96*, 307.
(33) Bender, R.; Braunstein, P.; Jud, J.-M.; Dusausoy, Y. *Inorg. Chem.* **1984**, *23*, 4489.

Scheme 4. Suggested Mechanism for the Formation of the Heterotetranuclear Clusters

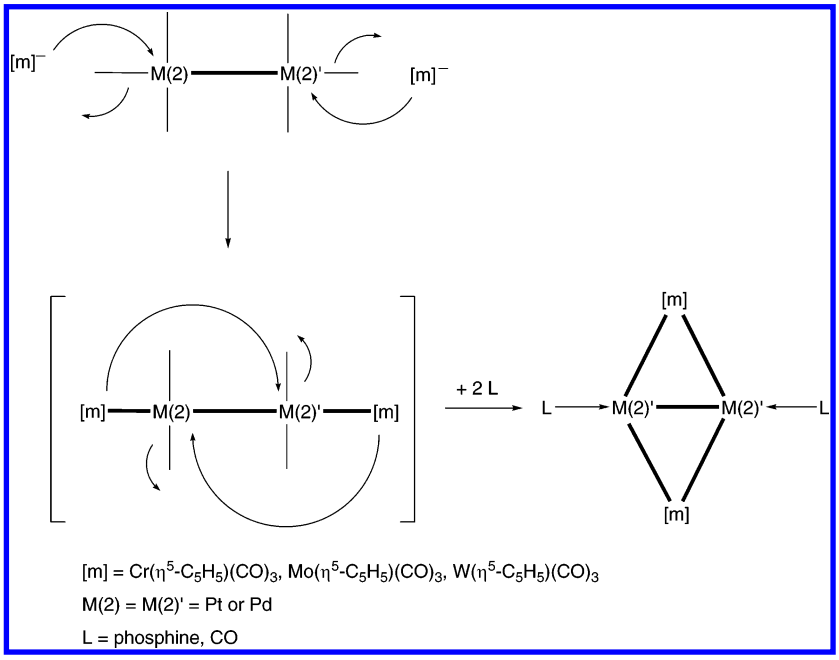

and **13**) and lead to the stable tetranuclear clusters (Scheme 4). It is interesting to note that similar deeply colored intermediates have also been observed in the reactions between carbonylmetalates $[m]^-$ and the d^9-d^9 precursor complex $[Pd_2(\mu\text{-dppm})_2Cl_2]$ and were suggested to have a linear metal core, $[m]-d^9-d^9-[m]$, which rearranges into a spike-triangular structure by insertion of the fragment [m] into a Pd−P bond.[34,35]

When the heterotetranuclear clusters discussed here are prepared from the d^8 mononuclear precursor complexes, *trans*-$[PtCl_2L_2]$ and *trans*-$[PdCl_2L_2]$ (L = PR_3, PhCN), it has been previously envisioned that a *trans*-[m]−Pt(or Pd)L_2−[m] chain complex is formed first.[3,33] When L = phosphine ligands, its instability resulting from the steric bulk of L (flat or rodlike L ligands give stable chain complexes), would result in homolytic cleavage of a [m]−Pt (or Pd) metal−metal bond and lead to two radical fragments $[m]^\bullet$ and $\{-[m]-Pt\ (or\ Pd)\}^\bullet$. Their homocoupling yields the [m]−[m] dinuclear complex and the $[m]_2$(Pd or $Pt)_2$ clusters.[3,33]

4. Syntheses of Mixed-Metal Complexes and Clusters from Heterodinuclear Precursors. We also envisioned the synthesis of heteropolymetallic Mo_2PdPt clusters with the hope of increasing the stability of the products by introducing Pt while maintaining the high reactivity characteristic of Pd derivatives.

Therefore, we examined the use of different mixed-metal Pd(I)−Pt(I) complexes as building blocks for cluster synthesis. A dinuclear complex such as $[PdPt(NCMe)_6](BF_4)_2$, which has not yet been described, would represent an excellent candidate, by analogy with its dipalladium analogue which led to the Mo_2Pd_2 structures. We attempted to synthesize it from $[Pd_2(dba)_3]$ and $[Pt(NCMe)_4](BF_4)_2$ and from $[Pt_2(dba)_3]$ and $[Pd(NCMe)_4](BF_4)_2$, but no reaction was observed.

However, when the stronger *tert*-butylisocyanide was used in place of the acetonitrile ligands, the reaction between 2 equiv of $[Pt(CNt\text{-}Bu)_4][PF_6]_2$ and $[Pd_2(dba)_3]$, followed by the addition of 4 equiv of *t*-BuNC in CH_2Cl_2, produced the new heterobimetallic complex $[PdPt(CNt\text{-}Bu)_6](PF_6)_2$ (**17**).

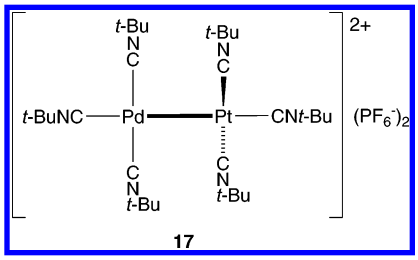

The reaction between Li·**9**·2DME and **17** in THF at −78 °C, after the reaction mixture was stirred overnight and the temperature brought to ambient, yielded a black precipitate of palladium metal and an orange compound that was isolated from the solution. It was not the expected tetranuclear cluster but the linear trinuclear complex *trans*-$[(\eta^5\text{-}C_5H_4NMe_2)_2(OC)_6Mo_2Pt(CNt\text{-}Bu)_2]$ (*Mo−Pt−Mo*) (**18**).[27]

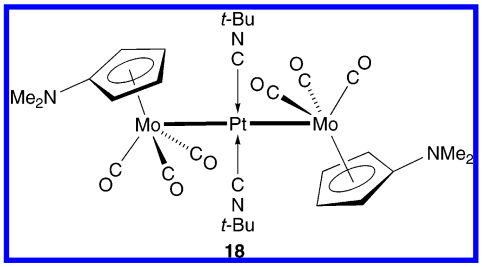

Isolation of this complex indicates that cleavage of the Pt−Pd bond in the precursor complex has occurred.

(34) Braunstein, P.; Guarino, N.; de Méric de Bellefon, C.; Richert, J. L. *Angew. Chem.* **1987**, *99*, 77; *Angew. Chem., Int. Ed. Engl.* **1987**, *26*, 88.

(35) Braunstein, P.; de Méric de Bellefon, C.; Ries, M. *Inorg. Chem.* **1988**, *27*, 1338.

The formation of this complex prompted us to use *trans*-$[PtCl_2(NCPh)_2]$ as a precursor, with the hope that displacement of the labile PhCN ligand could lead to a 2e−3c C_{ipsoCp}−N−Pt interaction. However, the heterometallic linear complex obtained as the major product, *trans*-$[(\eta^5\text{-}C_5H_4NMe_2)_2(OC)_6Mo_2Pt(NCPh)_2]$ (*Mo*−*Pt*−*Mo*) (**19**), did not show any interaction between the Cp-bound amino group and Pt.

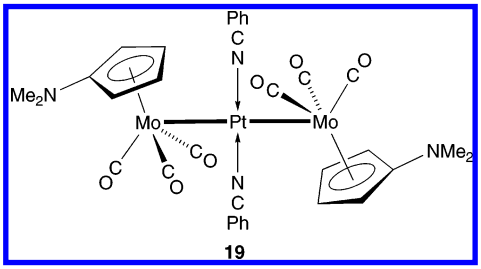

Formation of this complex was associated with smaller quantities of $[Mo_2Pt_2(\eta^5\text{-}C_5H_4NMe_2)_2(CO)_8]$ (**20**), $[(\eta^5\text{-}C_5H_4NMe_2)(OC)_3MoPt(NCPh)Cl]$ (*Mo*−*Pt*) (**21**), and $[Mo(\eta^5\text{-}C_5H_4NMe_2)(CO)_3Cl]$ (**22**).

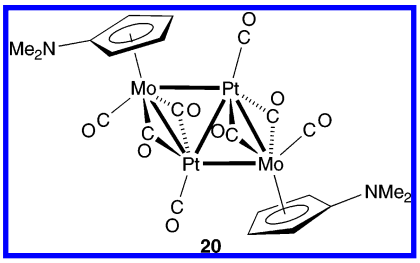

The synthesis of these compounds and the crystal structures of **19**, **21**, and **22** will be detailed elsewhere.[27]

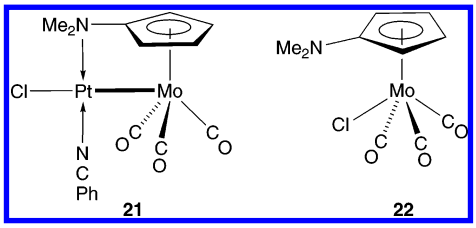

The crystal structure of the 58 CVE cluster **20** was also determined by X-ray diffraction. It adopts a planar triangulated geometry. Even if it is not a major product of the reaction, **20** is very interesting because it is the first Cp-containing cluster in this family to adopt such a geometry without any phosphine coordinated to platinum. The origin of the carbonyl ligands coordinated to platinum is to be found in the decomposition of some $Mo(\eta^5\text{-}C_5H_4NMe_2)(CO)_3$ fragments.

An ORTEP view of the structure of **20** is shown in Figure 7 with the main distances and angles. Its geometry differs from that of $[Mo_2Pt_2(\eta^5\text{-}C_5H_5)_2(CO)_6(PEt_3)_2]$,[33] each molybdenum being bonded to one terminal and two doubly bridging carbonyls. This arrangement is however similar to that of the carbonyls in clusters **4**, **12**, and **13**. The angle, β, between the mean plane of the amino-Cp and the metal plane is 89.7(2)° (see Table 1). The sum of the angles around N is 357(1)°.

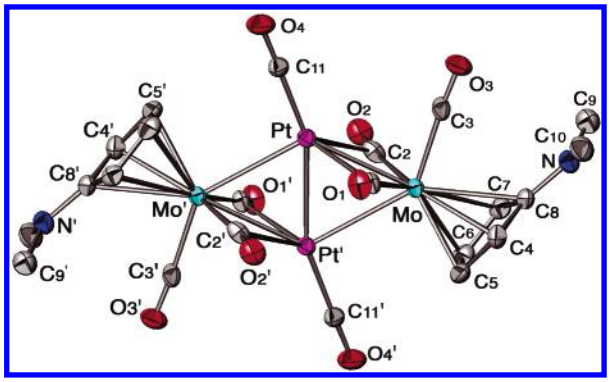

Figure 7. ORTEP view of the structure of **20** with the atom-numbering scheme. Thermal ellipsoids enclose 50% of the electron density. Selected bond distances (Å) and angles (deg): Pt−Pt′ = 2.6649(5), Pt−Mo = 2.7448(6), Pt′−Mo = 2.8388(6), Pt−C(11) = 1.865(7), Pt−C(1) = 2.452(7), Pt−C(2) = 2.319(7), Mo−C(1) = 2.009(8), Mo−C(2) = 2.041(7), Mo−C(3) = 2.024(7), C(1)−O(1) = 1.160(9), C(2)−O(2) = 1.155(8), C(3)−O(3) = 1.135(8), C(11)−O(4) = 1.127(8), C(8)−N = 1.357(9); Pt′−Pt−Mo = 63.28(2), Mo−Pt−Mo′ = 123.02(1), Pt−Pt′−Mo = 59.73(2), Pt−Mo−Pt′ = 56.99(1), Pt′−Pt−C(11) = 160.0(2), Mo−C(1)−O(1) = 167.6(6), Mo−C(2)−O(2) = 163.7(6), Mo−C(3)−O(3) = 176.2(6), Pt−C(1)−O(1) = 116.9(6), Pt−C(2)−O(2) = 118.2(5), Pt−C(11)−O(4) = 178.4(7), C(8)−N−C(9) = 119.9(6), C(8)−N−C(10) = 119.3(7), C(9)−N−C(10) = 117.4(6).

5. Structural Comparison of the Clusters Containing a Mo(π-ring)(CO)$_3$ Fragment. 5.1. Metal Cores. In all the clusters discussed here, the centrosymmetric metal core has the shape of a parallelogram. It is closest to a lozenge in **3b**,[3] **6**,[2] **11**, **15**, **16**, and **20** with the Mo−M(2) and Mo−M(2′) bond lengths being almost equal and longer than the M(2)−M(2′) distance. For **3b**, **6**,[2] **11** and **15**, the Pd−Pd′ distance ranges from 2.582(1) (in **3b**) to 2.5955(4) Å (in **6**), and the Mo−Pd distances range from 2.8075(5) (in **15**) to 2.8815(4) Å (in **6**). In **16** and **20**, the Pt−Pt′ distances are similar (2.650(2) and 2.6649(5) Å, respectively), while their Mo−Pt distances reflect a more regular rhombus in **16** (2.7739(8) and 2.826(2) Å) than in **20** (2.7448(6) and 2.8388(6) Å). The partial coordination of the Mo-bound π-ring to the palladium centers in clusters **12** and **13** results in a significant elongation of the Mo−Pd-bridged bond and in a shortening of the other Mo−Pd bond: the Mo−Pd bond lengths are 2.666(1) and 2.959(10) Å in **12** and 2.676(1) and 2.877(2) Å in **13**. These two clusters are therefore best described as adopting a parallelogram geometry. The nature of their π-ring significantly affects the Pd−Pd distances (2.892(1) and 3.015(1) Å, respectively). All these metal−metal distances are in the range found for the corresponding bonds in the literature.[36] Interestingly, the shape of the Re_2Pd_2 metal core of cluster **4**, which contains a "bridging" phenylborole ligand, is also closer to a parallelogram than to a lozenge, with Re−Pd distances of 2.666(1) and 2.866(1) Å. Its Pd−Pd′ distance of 2.899(2) Å is similar to that in **12**.[4]

5.2. Bonding and Orientation of the Mo(π-ring)(CO)$_3$ Fragments. The various tricarbonylmetalates $[Mo(\pi\text{-ring})(CO)_3]^-$ **1b**, **5a**, **5b**, **7**, **8**, and **9** used to prepare clusters are related to each other by the isolobal analogy (Scheme 5).

(36) Burrows, A. D.; Mingos, D. M. P. *Transition Met. Chem.* **1993**, *18*, 129.

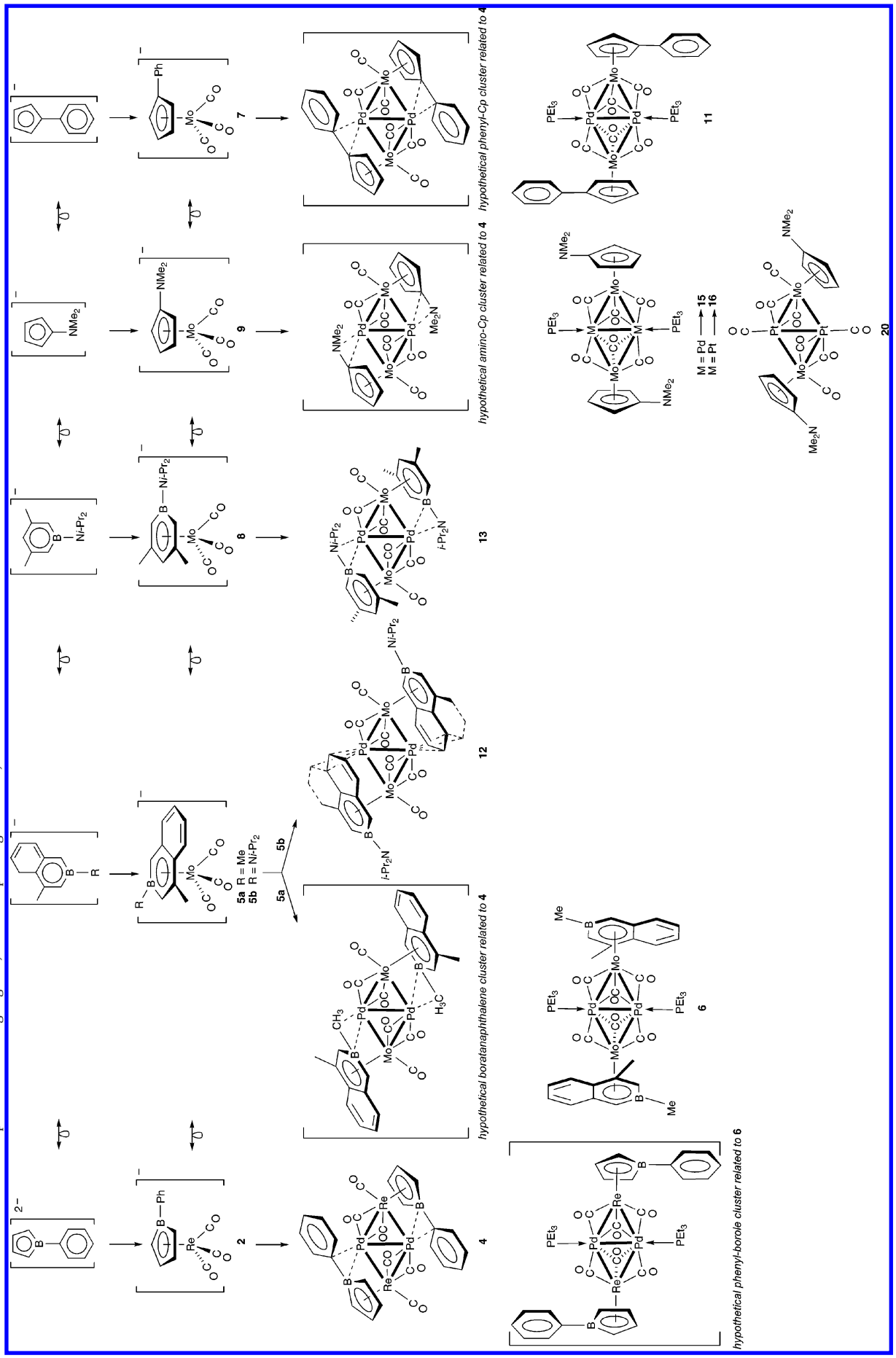

Scheme 5. Isolobal Relationships between π-ring Ligands, the Corresponding Metalates, and the Related Clusters

Because the Mo(π-ring)$(CO)_3$ building block is a recurrent entity in both the precursors and the products, a comparison of its bonding mode in the clusters is justified. In all these clusters, it adopts a bridging position toward a L → Pd−Pd ← L or L → Pt−Pt ← L central fragment, which involves the metal and the carbonyl ligands. Since a localized electron count around the metal atoms cannot be performed in these 58e clusters, we will consider the whole bridging moiety μ-[Mo(π-ring)$(CO)_3]^-$, as an anionic 18e moiety formally donating 4 electrons to the L → Pd(I)−Pd(I) ← L or L → Pt(I)−Pt(I) ← L (L → d^9−d^9 ← L) central unit (L = PEt_3, CO) in **3b**, **6**, **11**, **15**, **16**, and **20**. This is reminiscent of the situation encountered in a number of complexes containing a L → d^9−d^9 ← L unit bridged by more conventional 4e donor ligands (see Scheme 1). This provides the Mo and Pd or Pt centers with their usual electron count of 18e and 16e, respectively. In **12** and **13**, the anionic bridging building block μ-[Mo(π-ring)$(CO)_3]^-$ donates six electrons to the central Pd(I)−Pd(I) unit when the two additional electrons given by the pendant functional group of the π-ring are taken into account. The presence of five metal−metal bonds in all these clusters is consistent with their VEC of 58. The presence of isolobal Mo(π-ring)$(CO)_3$ building blocks in the Mo_2Pd_2 clusters facilitates a comparison of their orientation toward the central d^9−d^9 entity.

In the three-legged piano stool-type metalate [N*n*-Bu_4]-[Mo(η^5-C_5H_5)$(CO)_3$] (**23**),[37] the Mo$(CO)_3$ moiety is characterized by an almost perfect C_3 local symmetry axis, collinear with the C_5 axis C_{ring}−Mo.

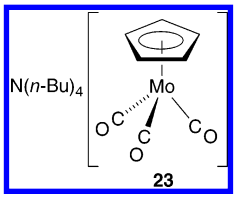

23

The three-legged piano stool environment observed in the Mo(π-ring)$(CO)_3$ building block is retained in **3b**, **6**,[2] **11**, **15**, and **16** but with a marked increase of the C−Mo−C angles corresponding to an opening of the "umbrella" formed by the three carbonyl ligands, which allows the Mo center to interact with both Pd or Pt atoms in an almost symmetrical fashion. The Mo−M(2) and the Mo−M(2)′ bonds are situated inside the cone defined by the three carbonyl legs of the piano stool. The average sum of the C(1)−Mo−C(2), C(1)−Mo−C(3), and C(2)−Mo-C(3) angles for these clusters (304(2)°) is much larger than the value calculated for **23** (264.2°). Consistently, the shortest average distance, *h* (Scheme 6), between the molybdenum atom and the plane defined by the carbon atoms of the three carbonyls is 0.88(1) Å against 1.14(1) Å in **23**.

Two geometrical parameters, β and γ, have been chosen to describe and compare the orientation of the whole bridging fragment, μ-[Mo(π-ring)$(CO)_3$], with respect to the metal core and the central d^9−d^9 axis in all the clusters described in this work. The angle β indicates the orientation of this fragment with respect to the metal core (Scheme 2). For the palladium clusters **3b**, **6**, **11**, and **15**, its value ranges from 74.7(1) (for **3b**) to 82.7(1)° (for **15**). In platinum cluster **16** the value of β is 86.3(3)°, which is slightly larger than those for **3b**, **6**, **11**, and **15** and close to 90°. This indicates that **16** is more symmetrical than these other phosphine-substituted clusters. These values are slightly smaller than in clusters **12**, **13**, and **20**, in which there is no phosphine coordinated to palladium or platinum (see below). The mean planes defined by the carbon atoms of the ring and the carbon atoms of the three carbonyls are almost parallel. The average value of the angle, δ, between these two planes is 4.6(1)°, which is close to the δ value of 1.95(10)° in **23** (see Table 1). This is also consistent with a conservation of the whole Mo(π-ring)$(CO)_3$ building block, since the parallelism between these two planes in the starting metalates is maintained in the final geometries. The angle, γ, between the axis passing through C_{ring} and C_{sym} and the M(2)M(2)′ axis (Scheme 2) reflects the tilt of the Mo(π-ring)$(CO)_3$ fragment with respect to the d^9−d^9 axis. The average value of 86.40(2)° for **3b**, **6**, **11**, **15**, and **16** indicates a highly symmetrical structure. The orientation of the Mo(π-ring)$(CO)_3$ fragment with respect to the d^9−d^9 unit determines the bonding mode of the carbonyl ligands in the clusters. It results in two semi-doubly bridging modes and one semi-triply bridging mode for the CO ligands for **3b**, **6**, **11**, and **15** and three semi-doubly bridging carbonyls for **16**. This is consistent with the values of the asymmetry parameter, α (Scheme 7),[38,39] ranging from 0.12 to 0.24. Consequently, the Mo−C(1)−O(1), Mo−C(2)−O(2), and Mo−C(3)−O(3) angles, which are much smaller than 180° (between 149.3(8) and 166.6(5)°), reflect the interactions between the palladium or platinum atoms and C(1)O(1), C(2)O(2), and C(3)O(3), respectively. The geometry of the [Mo(π-ring)$(CO)_3$] fragment in **3b**, **6**, **11**, **15**, and **16** is therefore best described as being of the three-legged piano stool type.

For clusters **4**, **12**, and **13**, the orientation of the M(1)(π-ring)$(CO)_3$ (M(1) = Mo, Re) fragment with respect to the

Scheme 6. Distance, *h*, between the Mo Atom and the Plane Defined by the Carbonyl C Atoms

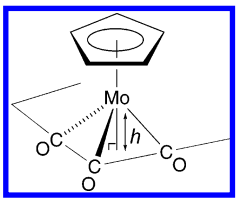

Scheme 7. $\alpha = (d_2 - d_1)/d_1$

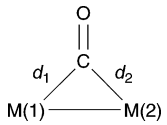

$0.1 \le \alpha \le 0.6$ = semi-bridging carbonyl; $\alpha \le 0.1$ = bridging carbonyl; $\alpha \ge 0.6$ = terminal carbonyl.

(37) Crotty, D. E.; Corey, E. R.; Anderson, T. J.; Glick, M. D.; Oliver, J. P. *Inorg. Chem.* **1977**, *16*, 920.

(38) Klingler, R. J.; Butler, W. M.; Curtis, M. D. *J. Am. Chem. Soc.* **1978**, *100*, 5034.

(39) Curtis, M. D.; Butler, W. M. *J. Organomet. Chem.* **1978**, *155*, 131.

d^9-d^9 axis is very different from that in **3b**, **6**, **11**, **15**, and **16** because of the interaction of the π-ring, or its substituent, with palladium. This is best illustrated by a decrease of the γ angle (between 68.33(4) and 74.72(2)° for **4**, **12**, and **13** versus 85.14(3) and 87.19(1)° for **3b**, **6**, **11**, **15**, and **16**). There is an opening of the "umbrella" formed by the three carbonyl ligands, as observed in clusters **3b**, **6**, **11**, **15**, and **16**. Consistently, the distance *h* in clusters **12** and **13** is 1.08(1) Å (versus 1.14(1) Å in **23**; Scheme 6 and Table 1). Contrary to the observation made for **3b**, **6**, **11**, **15**, and **16**, the three-legged piano stool environment in the M(1)(π-ring)$(CO)_3$ building block is not retained in **4**, **12**, and **13**. The M(1)−Pd′ bond is situated inside the cone defined by the three carbonyls legs of the piano stool, whereas the M(1)−Pd bond is situated outside the cone. This confers to these M(1) atoms a four-legged piano stool environment formed by the carbonyls and the Pd atom. The orientation of the $M(1)-C_{ring}$ axis, with respect to the Pd−Pd bond, confers a semi-doubly bridging bonding mode to two of the carbonyls and a terminal position to the third carbonyl. As a consequence, the M(1)−C(1)−O(1) and M(1)−C(2)−O(2) angles are smaller than 180° (between 161(1) and 163.7(5)°), sign of interactions between the palladium atoms and C(1)O(1) and C(2)O(2), respectively. Moreover, the α parameter (Scheme 4) for C(1)O(1) and C(2)O(2), between 0.11 and 0.15, is consistent with their semi-doubly bridging bonding mode in **4** and **12**. For **13**, α is smaller than 0.1 for both carbonyls (0.08 and 0.09), consistent with their doubly bridging bonding mode. The geometry of the M(1)(π-ring)$(CO)_3$ fragment in **4**, **12**, and **13** is therefore best described as being of the four-legged piano stool type.

Although the metal core of cluster **20** is similar to that of **3b**, **6**, **11**, **15**, and **16**, the orientation of the Mo(π-ring)$(CO)_3$ fragment with respect to the d^9-d^9 axis (Pt−Pt) (γ = 75.87(1)°) is intermediate between that in **3b**, **6**, **11**, **15**, and **16** (γ average value of 86.40(2)) and that in **4**, **12**, and **13** (γ average value of 70.68(2)°). Such differences in orientation appear to be associated to the value of the L−Pd−Pd or L−Pt−Pt angle, which is itself function of the steric bulk of L. The reasons for a value of only 160.0(2)° in **20** are not clear at this point. The π-ring mean plane in **20** is almost orthogonal to the metal plane (β = 89.7(2)°). The opening of the umbrella formed by the carbonyls is also observed for this cluster, and the distance *h* in this case is 1.02(1) Å, which is close to the values reported for clusters **4**, **12**, and **13**. The orientation of the $Mo-C_{ring}$ axis, with respect to the Pt−Pt bond, results in two semi-doubly bridging and one terminal carbonyls. As a consequence, the angles Mo−C(1)−O(1) (167.6(6)°) and Mo−C(2)−O(2) (163.7(6)°) are smaller than 180°, and the values of the parameter α (Scheme 4), 0.22 for C(1)O(1) and 0.14 for C(2)O(2), are consistent with their semi-doubly bridging bonding mode. In **20**, the geometry around the molybdenum is best described as a four-legged piano stool, similar to the geometries observed for **4**, **12**, and **13**.

Conclusion

In this work, we have provided an overview of the bonding behavior of isolobal tricarbonylmetalates building blocks containing boratanaphthalene (**5a** and **5b**), boratabenzene (**8**), and cyclopentadienyl (**7** and **9**) π-bonded ligands, toward a central dinuclear d^9-d^9 fragment in the 58 CVE tetranuclear clusters **3b**, **6**, **11**, **12**, **13**, **15**, **16**, and **20**. These relationships are summarized in Scheme 5 which shows some obvious similarities but also significant differences between the structures of the resulting heterotetranuclear clusters. Similar to cluster **3b**, the new clusters **11**, **15**, **16**, and **20** contain a substituted cyclopentadienyl ring, whose pendant functional group does not interact with the neighboring palladium or platinum centers, even with the good electron-donor amino group. Each Mo(π-ring)$(CO)_3$ building block behaves as an anionic 4-electron donor toward the central d^9-d^9 fragment, and the coordination sphere around the palladium or platinum is completed by phosphine (**11**, **15**, and **16**) or carbonyl ligands (**20**). The amino-boratanaphthalene ring in cluster **12** is connected to the palladium through the π-system of the aromatic ligand and not through the amino group, whereas in **13**, the coordination of the amino-boratabenzene group with palladium takes place through a 2e−3c B−N−Pd interaction. In **12** and **13**, each 18e anionic [Mo(π-ring)$(CO)_3]^-$ structural entity brings 4 electrons to the central d^9-d^9 fragment and two additional electrons through the coordination of the functional group of the π-ring with palladium. Geometry differences have been observed and discussed for this family of heterometallic clusters, dependent on the presence or absence of coordination between the π-ring and the d^9 center.

Under similar reaction conditions, the isolobal boratanaphthalene-, boratabenzene-, and cyclopentadienyl-containing metalates lead to similar tetranuclear triangulated clusters. Except in the case of the boratanaphthalene cluster **6**, of which the geometry is very similar to that of the Cp-containing clusters (**3b**, **11**, **15**, **16**, and **20**), the presence of a boron atom in the π-bonded ligand tends to result in additional ligand interactions with the adjacent metal center (**12** and **13**). Related coordination modes with the Cp-containing metalloligands were not found.

These studies, aimed at a systematic comparison between organometallic building blocks used in heterometallic cluster synthesis, provide a better understanding of the relationship between the cluster total electron count, the nature of the building blocks, and the molecular structures. When the applications of the planar M_2Pd_2 clusters in homogeneous catalysis (hydrogenation of alkenes and alkynes, oligomerization of butadiene, photochemical hydrosilations of alkenes, and very recently, cross-coupling reactions of aryl halides and triflates with 13-metal alkylating reagents)[40−42] and in heterogeneous catalysis (carbonylation of organic nitro

(40) Braunstein, P.; Rosé, J. In *Metal Clusters in Chemistry*; Braunstein, P., Oro, L. A., Raithby, P. R., Eds.; Wiley-VCH: Weinheim, Germany, 1999; Vol. 2, p 616.
(41) Pittman, C. U., Jr.; Honnick, W.; Absi-Halabi, M. m.; Richmond, M. G.; Bender, R.; Braunstein, P. *J. Mol. Catal.* **1985**, *32*, 177.
(42) Shenglof, M.; Molander, G. A.; Blum, J. *Synthesis* **2006**, *1*, 111.

derivatives into isocyanates, catalytic reduction of NO, and olefin hydrogenation)[40,43−47] are considered, the new related clusters described in this work may also reveal an interesting potential for applications.

Experimental Section

General Procedures. Reactions were carried out under a nitrogen atmosphere using conventional Schlenk techniques. Solvents were dried according to standard procedures. Elemental analyses were performed by the Service de Microanalyses, Université Louis Pasteur, Strasbourg, France.

NMR spectra were recorded on a Bruker Avance 400 (^{11}B, 128.34 MHz; ^{15}N, 40.56 MHz) and a Bruker Avance 300 (^{1}H, 300 MHz; ^{13}C{^{1}H}, 75.47 MHz; ^{31}P{^{1}H}, 121.49 MHz). Chemical shifts (in ppm) were measured at ambient temperature and are referenced to external TMS for ^{1}H and ^{13}C, $NaBH_4$ for ^{11}B, H_3PO_4 (84%) for ^{31}P, and DMF for ^{15}N. The spectra were measured at 298 K. Assignments are based on APT and DEPT spectra and ^{1}H, ^{1}H-COSY, and ^{1}H,^{13}C-HMQC experiments. The IR spectra were recorded in the region of 4000−400 cm^{-1} on a FT-IR IFS66 Bruker spectrometer. ESI mass spectra were recorded on an Bruker micrOTOF mass spectrometer.

The following compounds were synthesized according to literature procedures or improved syntheses: C_5H_5Ph,[23] *trans*-[$PdCl_2(NCPh)_2$],[48] [$Pd_2(NCMe)_6](BF_4)_2$,[24] *trans*-[$PdCl_2(PEt_3)_2$],[48] *trans*-[$PtCl_2(PEt_3)_2$],[48] [$Pt(CN\textit{t}\text{-}Bu)_4](PF_6)_2$,[49] [$Pd_2(dba)_3$]·$CHCl_3$, *trans*-[$PtCl_2(NCPh)_2$],[48] Li[$Mo(\eta^5\text{-}2,4\text{-}MeC_9H_6BN\textit{i}\text{-}Pr_2)(CO)_3$],[2] Li[$Mo(\eta^5\text{-}C_5H_4NMe_2)(CO)_3$],[27] and Li[$Mo(\eta^5\text{-}C_5H_3Me_2BN\textit{i}\text{-}Pr_2)(CO)_3$].[27]

Preparation of Na[$Mo(\eta^5\text{-}C_5H_4Ph)(CO)_3$]·2DME (7). Freshly distilled phenylcyclopentadiene (2.50 g, 17.6 mmol) was dissolved into 100 mL of dry ice-cold THF and added slowly to a stirred suspension of an excess of sodium hydride (0.50 g, 20.8 mmol) in 50 mL THF kept at −78 °C. This solution was stirred at −30 °C until disappearance of the hydrogen bubbles. The mixture was filtered through Celite, giving a light orange solution of $Na(C_5H_4Ph)$. Solid [$Mo(CO)_6$] (4.64 g, 17.6 mmol) was added to this solution, and the mixture was kept at reflux overnight, cooled to room temperature, concentrated to 50 mL, and precipitated by the addition of cold pentane (200 mL). The supernatant was removed by filtration, leaving a brown powder which was washed twice with pentane (50 mL) and dried in vacuo for 4 h. Yield of Na·**7**·(2DME): 6.62 g, 72% (12.6 mmol). The product is sensitive to air and humidity, insoluble in hexane and pentane and soluble in THF. It has been characterized by IR spectroscopy. IR (DME): ν(CO) 1898s, 1792s, 1755m cm^{-1}.

Reaction of Na·7·2DME with *trans*-[$PdCl_2(NCPh)_2$] and Formation of [$Mo(\eta^5\text{-}C_5H_4Ph)(CO)_3]_2$ (10). Solid *trans*-[$PdCl_2(NCPh)_2$] (0.41 g, 1.08 mmol) was added to a stirred solution of Na·**7**·2DME (1.13 g, 2.15 mmol) in toluene (50 mL) cooled with dry ice (−78 °C). The solution immediately turned dark blue and was stirred for 0.5 h at −78 °C. The mixture was evaporated to dryness at room temperature; meanwhile, it became dark brown. The black residue was chromatographed on an alumina column. Elution with toluene gave a red compound, which was crystallized from toluene/pentane and identified as [$Mo(\eta^5\text{-}C_5H_4Ph)(CO)_3]_2$ (**10**) (0.28 g, 0.44 mmol, 41%). It has been characterized by IR, X-ray crystallography, and elemental analysis. Anal. Calcd for $C_{28}H_{18}Mo_2O_6$: C, 52.36; H, 2.82. Found: C, 52.55 H, 2.95%. IR (KBr): ν(CO) 1950s, 1920sh, 1899sh, 1886s cm^{-1}. IR (CH_2Cl_2): ν(CO) 2012w, 1958s, 1912br m cm^{-1}. Further elution with toluene and THF produced no other compounds leaving an important amount of dark residue on the top of the column.

Preparation of [$Mo_2Pd_2(\eta^5\text{-}C_5H_4Ph)_2(CO)_6(PEt_3)_2$] (11). Method A. Solid *trans*-[$PdCl_2(PEt_3)_2$] (0.50 g, 1.21 mmol) was added to a stirred solution of Na·**7**·2DME (1.27 g, 2.42 mmol) in toluene (50 mL) at room temperature. The solution turned dark blue immediately, stirring was maintained for 1 h, and the solvent was evaporated to dryness. The black residue was chromatographed on a alumina column. Elution with toluene/pentane (1:1) gave a red compound identified by IR as **10**. Elution with toluene afforded a dark-blue compound, recrystallized from toluene/pentane and identified as [$Mo_2Pd_2(\eta^5\text{-}C_5H_4Ph)_2(CO)_6(PEt_3)_2$] (**11**) (0.28 g, 0.26 mmol, 43% based on Pd). It has been characterized by IR, ^{1}H, ^{13}C{^{1}H}, and ^{31}P{^{1}H} NMR, X-ray crystallography, and elemental analysis. Anal. Calcd. for $C_{40}H_{48}Mo_2O_6P_2Pd_2$: C, 44.02; H, 4.43. Found: C, 43.78; H, 4.06%. IR (KBr): ν(CO) 1840s, 1807m, 1793sh, 1761m cm^{-1}. IR (CH_2Cl_2): ν(CO) 1832s, 1795sh, 1775m cm^{-1}. ^{1}H NMR(CD_2Cl_2): δ 7.44−7.16 (m, 10H, C_6H_5), AA′XX′ spin system 5.64 and 5.27 (2 pseudotriplets, 8H, Cp), 1.49 (m, 12H, PCH_2CH_3), 0.81 (m, 18H, PCH_2CH_3). ^{13}C{^{1}H} NMR (CD_2Cl_2): δ 241.6 (CO), 133.7−125.9 (Ph), 109.3 (1-C, π-C_5H_4), 90.3 (2-C, π-C_5H_4) 89.1 (3-C, π-C_5H_4), 16.9 (virtual t, PCH_2CH_3, $|^1J(PC) + {}^4J(PC)| = 20$ Hz), 8.2 (s, PCH_2CH_3). ^{31}P{^{1}H} NMR (CD_2Cl_2): δ 20.9.

Method B. Solid [$Pd_2(NCMe)_6](BF_4)_2$ (0.38 g, 0.60 mmol) was added to a stirred solution of Na·**7**·2DME (0.66 g, 1.25 mmol) in toluene (50 mL) cooled with dry ice (−78 °C). The solution turned dark blue within 1 h, and PEt_3 (180 μl, 1.22 mmol) was added to the cold mixture. The solution turned dark violet immediately; it was stirred for 15 min and filtered through a Celite pad until the solution was light blue. The solution was concentrated, and the dark crystals obtained from pentane were identified as **11** (0.59 g, 0.54 mmol, 90% based on Pd).

Preparation of [$Mo_2Pd_2(\eta^5\text{-}2,4\text{-}MeC_9H_6BN\textit{i}\text{-}Pr_2)_2(CO)_6$] (12). Solid [$Pd_2(NCMe)_6](BF_4)_2$ (0.63 g, 1.0 mmol) was added to a stirred solution of Li·**5b**·2DME (1.21 g, 2.0 mmol) in toluene (50 mL) cooled with dry ice (−78 °C). The solution turned dark blue; then it was stirred for 1 h and filtered through a Celite pad which had been prewashed with toluene. The solution was concentrated and chromatographed on an alumina column. Elution with toluene/pentane (1:1) produced two close bands. First, a violet band gave the meso (R,S) diastereoisomer, identified notably by single-crystal X-ray diffraction as **12** (0.32 g, 0.30 mmol, 30% based on Pd). Anal. Calcd for $C_{38}H_{46}B_2Mo_2N_2O_6Pd_2$: C, 43.34; H, 4.40; N, 2.66. Found: C, 43.08; H, 4.16; N, 2.94%. IR (CH_2Cl_2): ν(CO) 1961s, 1880w, 1842s cm^{-1}. Clear NMR spectra could not be successfully recorded because of the presence of paramagnetic residues. The second, a dark blue band, has been identified only by IR since the compound decomposed quickly, and ^{1}H NMR spectra could not be successfully recorded. IR (CH_2Cl_2): ν(CO) 1935s, 1877sh, 1845s cm^{-1}.

(43) Braunstein, P.; Bender, R.; Kervennal, J. *Organometallics* **1982**, *1*, 1236.
(44) Kawi, S.; Alexeev, O.; Shelef, M.; Gates, B. C. *J. Phys. Chem. B* **1995**, *99*, 6926.
(45) Hoost, T. E.; Graham, G. W.; Shelef, M.; Alexeev, O.; Gates, B. C. *Catal. Lett.* **1996**, *38*, 57.
(46) Kervennal, J.; Cognion, J.-M.; Braunstein, P. French Patent 2 515 640, 1981; U.S. Patent 4478,757, 1982; *Chem. Abstr.* **1982**, *99*, 139487.
(47) Carrion, M. C.; Manzano, B. R.; Jalon, F. A.; Maireles-Torres, P.; Rodriguez-Castellon, E.; Jimenez-Lopez, A. *J. Mol. Catal. A* **2006**, *252*, 31.
(48) Hartley, F. R. *Organomet. Chem. Rev. A* **1970**, *6*, 119.
(49) Lai, S.-W.; Chan, M. C. W.; Wang, Y.; Lam, H. W.; Peng, S. M.; Che, C. M. *J. Organomet. Chem.* **2001**, *617−618*, 133.

Preparation of $[Mo_2Pd_2(\eta^5\text{-}3,5\text{-}Me_2C_5H_3BN\textit{i}\text{-}Pr_2)_2(CO)_6]$ (13). Method A. Solid *trans*-$[PdCl_2(NCPh)_2]$ (0.23 g, 0.61 mmol) was added to a stirred solution of Li·**8**·2DME (0.74 g, 1.23 mmol) in toluene (30 mL) cooled with dry ice (−78 °C). The solution immediately turned dark blue; then it was stirred for 1 h and evaporated to dryness. The black residue was chromatographed on an alumina column. Elution with toluene gave a dark blue compound, which was recrystallized from toluene/pentane and identified as $[Mo_2Pd_2(\eta^5\text{-}3,5\text{-}Me_2C_5H_3BN\textit{i}\text{-}Pr_2)_2(CO)_6]$ (**13**) (0.13 g, 0.13 mmol, 43% based on Pd). It has been characterized by IR, ^{1}H, ^{11}B, and ^{15}N (inverse detection) NMR, X-ray crystallography, and elemental analysis. Anal. Calcd for $C_{32}H_{46}B_2Mo_2N_2O_6Pd_2$: C, 39.18; H, 4.73. Found: C, 39.47; H, 4.82%. IR (KBr): ν(CO) 1922s, 1850s cm^{-1}. IR (CH_2Cl_2): ν(CO) 1925s, 1841s cm^{-1}. ^{1}H NMR (CD_2Cl_2): δ 5.82 (br s (couplings have not been observed), 2H, 4-H), 4.23 (br s (couplings have not been observed), 4H, 2-/6-H), 3.62 (sept, ^3J = 6.6 Hz, 4H, NCH), 2.10 (s, 12H, 3-/5-Me), 1.41 (d, ^3J = 6.6 Hz, Me-*i*Pr), 1.33 (d, ^3J = 6.6 Hz, Me-*i*Pr). ^{11}B-{^{1}H} NMR: δ 48.72. ^{15}N NMR (inverse detection): δ −308.5.

Method B. Solid $[Pd_2(NCMe)_6](BF_4)_2$ (0.39 g, 0.62 mmol) was added to a stirred solution of Li·**8**·2DME (0.74 g, 1.23 mmol) in toluene (30 mL) cooled with dry ice (−78 °C). The solution turned dark blue; then it was stirred for 1 h and then filtered through a Celite pad. The solution was concentrated and crystallized from pentane to obtain dark crystals of **13** (0.54 g, 0.55 mmol, 89% based on Pd).

Preparation of $[Mo_2Pd_2(\eta^5\text{-}C_5H_4NMe_2)_2(CO)_6(PEt_3)_2]$ (15). A suspension of $[Pd_2(NCMe)_6][BF_4]_2$ (0.21 g, 0.33 mmol) in THF (5 mL) was added to a stirred solution of Li·**9**·2DME (0.31 g, 0.66 mmol) in THF (20 mL) at −78 °C. The solution immediately turned dark blue. Triethylphosphine (98 μl, 0.66 mmol, d = 0.802) was added to the solution, which then turned violet. Under constant stirring, the temperature was slowly increased to room temperature in 3 h. The resulting dark violet mixture was evaporated to dryness, washed with pentane, and purified by crystallization from a CH_2Cl_2/heptane mixture. Dark violet crystals of **15** were obtained and characterized by single-crystal X-ray diffraction. Purification by column chromatography (silica gel pretreated with NEt_3, toluene, and then THF/pentane) led to lower yields because of the retention of the cluster on the support. Yield: 0.14 g, 41% based on Pd after recrystallization from CH_2Cl_2/heptane. It has been characterized by IR, ^{1}H, ^{31}P, and ^{13}C NMR, X-ray crystallography, electrospray mass spectrometry, and elemental analysis. Anal. Calcd for $C_{32}H_{50}Mo_2N_2O_6P_2Pd_2$: C, 37.48; H, 4.91; N, 2.73. Found: C, 37.26; H, 4.84, N, 2.58%. IR (KBr): ν(CO) 1875vw, 1826vs, 1750s cm^{-1}. ^{1}H NMR (C_6D_6): δ AA′MM′ system 4.88 and 4.37 (2 pseudo-triplets, 8H, Cp), 2.36 (s, 12H, NMe_2), 1.71 (m, 12H, PCH_2), 0.99 (m, 18H, PCH_2CH_3). ^{13}C{^{1}H} NMR (C_6D_6): δ 242.9 (CO), 83.2 (Cp), 70.3 (Cp), 39.7 ($CpNMe_2$), 17.2 (virtual t, PCH_2CH_3, $|^1J$(PC) + ^4J(PC)| = 20 Hz), 8.1 (s, PCH_2CH_3) (C_{ipso} was not observed).^{31}P-{^{1}H} NMR (C_6D_6): δ 18.9. MS (ES): m/z (I_{rel}) 1287 (M^+− 2CO, 50%).

Preparation of $[Mo_2Pt_2(\eta^5\text{-}C_5H_4NMe_2)_2(CO)_6(PEt_3)_2]$ (16). A suspension of *trans*-$[PtCl_2(PEt_3)_2]$ (0.28 g, 0.56 mmol) in THF (10 mL) was added to a stirred solution of Li·**9**·2DME (0.53 g, 1.12 mmol) in THF (20 mL) at room temperature. After it was stirred for 2 h, the mixture was filtered, and the solvent was removed in vacuo. The residue was chromatographed on an alumina column. Elution with toluene gave a red solution of **14** (trace amount), followed by an orange solution (trace amount) which was not identified. Cluster **14** was identified by IR spectroscopy and by comparison with the corresponding compound with the Cp ligand in place of $CpNMe_2$. Elution with a THF/pentane mixture (1:5) gave a violet solution of **16** (0.026 g, 0.022 mmol). Violet crystals were obtained from THF/pentane. Yield: 8%. It has been characterized by IR, ^{1}H and ^{31}P NMR, X-ray crystallography, and elemental analysis. Anal. Calcd for $C_{32}H_{50}Mo_2N_2O_6P_2Pt_2$: C, 31.96; H, 4.19; N, 2.33. Found: C, 31.21; H, 4.01; N, 2.30%. IR (KBr): ν(CO) 1832sh, 1798s, 1706s br cm^{-1}. ^{1}H NMR ($CDCl_3$): δ AA′MM′ system 4.97 and 4.43 (2 pseudo triplets, 8H, Cp), 2.63 (s, 12H, Me), 1.88 (m, 12H, PCH_2), 0.99 (m, 18H, PCH_2CH_3). ^{31}P{^{1}H} NMR ($CDCl_3$): δ 39.0 (s with ^{195}Pt satellites, ^1J(PtP) = 4323 Hz).

Preparation of $[PdPt(CN\textit{t}\text{-}Bu)_6](PF_6^-)_2$ (17). $[Pd_2(dba)_3]\cdot CHCl_3$ (0.24 g, 0.23 mmol) in CH_2Cl_2 (20 mL) and *t*-BuNC (0.076 g, 104

Table 2. Crystallographic Data, Data Collection Parameters, and Refinement Results

	10	**11**	**12**	**13**
formula	$C_{28}H_{18}Mo_2O_6$	$C_{40}H_{48}Mo_2O_6P_2Pd_2$	$C_{38}H_{46}B_2Mo_2N_2O_6Pd_2$	$C_{32}H_{46}B_2Mo_2N_2O_6Pd_2$
fw	642.30	1091.40	1053.07	981.01
cryst syst	orthorhombic	monoclinic	triclinic	monoclinic
space group	*Pbca*	$P2_1/c$	$P\bar{1}$	$P2_1/n$
a (Å)	7.577(5)	10.9789(10)	8.833(2)	8.352(5)
b (Å)	12.608(5)	14.453(2)	10.101(4)	20.035(5)
c (Å)	25.024(5)	13.274(2)	12.733(5)	10.811(5)
α (deg)	90.00	90.00	75.444(5)	90.00
β (deg)	90.00	105.73(5)	89.467(5)	103.05(5)
γ (deg)	90.00	90.00	67.042(5)	90.00
V (Å^3)	2390.6(19)	2027.4(7)	1007.5(6)	1762.3(14)
Z	4	2	1	2
cryst size (mm^3)	0.08 × 0.07 × 0.06	0.10 × 0.09 × 0.08	0.11 × 0.10 × 0.09	0.08 × 0.07 × 0.06
color	red	violet	green	green
D_{calcd} (g cm^{-3})	1.785	1.788	1.736	1.849
μ (mm^{-1})	1.092	1.600	1.532	1.744
T (K)	173(2)	173(2)	173(2)	173(2)
F(000)	1272	1084	522	972
Θ limits (deg)	2.29/27.47	2.39/29.95	3.15/33.16	2.81/50.44
no. of data measured	2732	5865	7646	18 127
no. of data ($I > 2\sigma(I)$)	1771	3259	5167	12226
no. of params	163	235	251	208
R1	0.0271	0.0866	0.0516	0.0444
wR2	0.0719	0.1087	0.1207	0.1410
GOF	0.672	1.100	0.929	1.078
max/min residual density (e Å^{-3})	0.690/−0.946	1.125/−1.559	0.973/−1.818	1.166/−1.504

	15	**16**	**20**
formula	$C_{32}H_{50}Mo_2N_2O_6P_2Pd_2$	$C_{32}H_{50}Mo_2N_2O_6P_2Pt_2$	$C_{22}H_{20}Mo_2N_2O_8Pt_2$
fw	1025.36	1202.74	1022.46
cryst syst	triclinic	triclinic	triclinic
space group	$P\bar{1}$	$P\bar{1}$	$P\bar{1}$
a (Å)	9.208(1)	8.9590(10)	8.1580(2)
b (Å)	9.938(1)	10.1280(10)	8.6250(3)
c (Å)	11.061(1)	11.0770(10)	9.9960(3)
α (deg)	106.08(5)	108.28(5)	78.1200(15)
β (deg)	99.15(5)	97.83(5)	67.7900(12)
γ (deg)	102.49(5)	101.97(5)	74.370(2)
V (Å^3)	923.35(16)	911.43(16)	622.80(3)
Z	1	1	1
cryst size (mm^3)	0.12 × 0.10 × 0.08	0.07 × 0.07 × 0.07	0.09 × 0.09 × 0.09
color	violet	violet	orange
D_{calcd} (g cm^{-3})	1.844	2.191	2.726
μ (mm^{-1})	1.752	8.454	12.229
T (K)	173(2)	173(2)	173(2)
F(000)	510	574	470
Θ limits (deg)	2.33/30.05	3.26/30.18	2.22/30.06
no. of data measured	5185	5286	3650
no. of data ($I > 2\sigma(I)$)	4039	4338	2911
no. of params	208	208	163
R1	0.0355	0.0623	0.0420
wR2	0.1016	0.1465	0.0961
GOF	1.044	1.050	0.982
max/min residual density (e Å^{-3})	1.053/−1.480	2.228/−2.855	2.509/−3.237

μl, $d = 0.735$, 0.92 mmol) were added to a solution of [Pt(CN*t*-Bu)$_4$](PF$_6$)$_2$ (0.37 g, 0.46 mmol) in CH_3CN (20 mL). After the reaction mixture was stirred for 1 h, the yellow solution was evaporated under reduced pressure, and a yellow solid **17** was precipitated with ether (100 mL), filtered, and washed with ether (3 × 10 mL) (0.47 g, 94%). It has been characterized by IR, ^{1}H NMR, and elemental analysis. Anal. Calcd for $C_{30}H_{54}F_{12}N_6P_2PdPt$: C, 33.05; H, 4.99; N, 7.71. Found: C, 33.32; H, 4.94; N, 8.03%. IR (KBr): ν(NC) 2202 vs. ^{1}H NMR (CD_3CN): δ 1.62 (s), 1.57 (s).

Crystal Structure Determinations. The data collections were performed on a Nonius Kappa-CCD area detector diffractometer (Mo Kα, $\lambda = 0.71070$ Å, φ scan). The relevant data are summarized in Table 2. The cell parameters were determined from reflections taken from one set of 10 frames (1.0° steps in φ angle), each at a 20 s exposure. The structures were solved using direct methods (SHELXS97) and refined against F^2 using the SHELXL97 software. The absorption was corrected empirically (with Sortav) for the area-detector data. All non-hydrogen atoms were refined with anisotropic parameters. The hydrogen atoms were included in their calculated positions and refined with a riding model in SHELXL97.

Acknowledgment. Dedicated to Prof. F. Mathey on the occasion of his 65th birthday, with our warmest wishes. The work was supported by the Ministery of Research (PhD grants to N.A. and P.C.), the CNRS and the Franco-German Research Training Group (GRK 532 of the DFG). We are grateful to Prof. G. E. Herberich (Aachen, German) for samples of Li[Mo(η^5-C$_5$H$_3$Me$_2$BN*i*-Pr$_2$)(CO)$_3$] and Li[Mo(η^5-2,4-MeC$_9$H$_6$BN*i*-Pr$_2$)(CO)$_3$] and to Dr. A. DeCian for the collection of the X-ray data.

Supporting Information Available: X-ray crystallographic files in CIF format and ORTEP views of the structures. This material is available free of charge via the Internet at http://pubs.acs.org. Crystallographic data can be obtained from the Cambridge Crystallographic Data Centre (CCDC606696−606702).

IC060318D